

Trends in Ecology & Evolution

 CellPress
OPEN ACCESS

Opinion

Linking biodiversity, ecosystem function, and Nature's contributions to people: a macroecological energy flux perspective

Ana Carolina Antunes ,^{1,2,*} Emilio Berti,^{1,2} Ulrich Brose,^{1,2} Myriam R. Hirt,^{1,2} Dirk N. Karger,³ Louise M.J. O'Connor,⁴ Laura J. Pollock,⁵ Wilfried Thuiller,⁴ and Benoit Gauzens^{1,2}

At macroecological scales, the provision of Nature's contributions to people (NCP) is mostly estimated with biophysical information, ignoring the ecological processes underlying them. This hinders our ability to properly quantify the impact of declining biodiversity and the provision of NCP. Here, we propose a framework that combines local-scale food web energy flux approaches and large-scale biodiversity models to evaluate ecosystem functions and flux-related NCP at extensive spatiotemporal scales. Importantly, this approach has the potential to upscale ecosystem functions, assess the vulnerability of flux-related NCP to the climate crisis, and support the development of multiscale mitigation policies.

From communities to ecosystem functions and Nature's contributions to people

The functioning of ecosystems is highly susceptible to changes in biodiversity and community composition induced by species invasions, extreme and long-term climatic changes, and anthropogenic disturbances [1]. As such, it becomes urgent to better understand how the response of ecosystems to perturbations at the community level will affect ecosystem functioning and, ultimately, **NCP** (see [Glossary](#)). Food web theory and the distribution of energy fluxes among species can be used to form mechanistic links among perturbations, biodiversity, community structure, and **ecosystem functions** [2–4]. Interestingly, the concept of energy flux could also be applied to estimate some potential NCP (hereafter referred to as '**flux-related NCP**') and better integrate ecological processes into the provision of NCP. The set of potential NCP that can be estimated through this approach is related to community-level processes that directly depend on interspecific interactions, such as regulation of detrimental organisms or food production (see [Table 1](#) and following section for correspondences between energy fluxes and flux-related NCP). For instance, in the Baltic Sea, community shifts led to a massive change in fish harvest, both in terms of species and biomass extracted [5], mirrored by shifts in energy fluxes [6]. As such, **food web models** can help reveal the causal mechanisms between environmental drivers, multi-species response, ecosystem functioning, and the associated supply of NCP [7].

Uncertainty about the future of NCP requires reliable models capable of predicting ecosystem functions and NCP changes at large spatial scales [8,9] for different scenarios of global change. However, due to the complexity of processes and interactions that determine ecosystem functioning in response to global change, most approaches that aim to evaluate ecosystem functions are often very context specific and usually applied at regional spatial scales [3]. This hinders progress toward estimating ecosystem functions and the supply of flux-related NCP across larger spatial scales and highly dynamic landscapes [10,11]. Useful tools for assessing NCP at macroecological scales have been developed over the past 20 years, mostly based on

Highlights

Evaluating and mapping ecosystem functions and associated Nature's contributions to people (NCP) across large spatial scales is complex.

One particular and often overlooked challenge is to integrate community-level processes, such as species interactions, into the evaluation of flux-related NCP supply, especially when working at macroecological scales.

This flux-related NCP evaluation could greatly benefit from advances in food web theory and statistical biodiversity modeling, which could simultaneously improve our understanding of the trophic interactions in ecological networks and the prediction of biodiversity across time and space while accounting for abiotic drivers (climate and land use).

We propose a macroecological framework that integrates biodiversity models and energy flux theory to upscale ecosystem functions and predicts the associated supply of flux-related NCP.

¹Institute of Biodiversity, Friedrich Schiller University Jena, Jena, Germany

²EcoNetLab, German Centre for Integrative Biodiversity Research (iDiv) Halle-Jena-Leipzig, Puschstrasse 4, 04103 Leipzig, Germany

³Swiss Federal Institute for Forest, Snow, and Landscape Research, 8903 Birmensdorf, Switzerland

⁴University of Grenoble Alpes, University of Savoie Mont Blanc, CNRS, LECA, F-38000 Grenoble, France

Table 1. A diversity of contributions delivered by nature to people can be directly related to individual energy fluxes or summed network fluxes^a

| Categories of NCP ^b (IPBES) | NCP | Link indicator (sum of energy fluxes) |
|---|-----------------------------------|--|
| Pollination and dispersal of seeds and other propagules | Pollination | Fluxes between plant and pollinator |
| | Seed dispersal | Fluxes between plant and seed disperser |
| Regulation of climate | Carbon sequestration | Fluxes to primary producers |
| Formation, protection, and decontamination of soils and sediments | Nutrient cycling (mineralization) | Nonassimilated flux to decomposers (1–assimilation efficiency) |
| | Nutrient cycling (decomposition) | Influx to decomposers |
| Regulation of detrimental organisms and biological processes | Pest regulation | Fluxes between pest and predator species (predation pressure) standardized per biomass of pest species |
| | Control of species invasion | Fluxes between invasive species and resource |
| | Disease control (vector control) | Fluxes between vector and predator |
| | Carcass removal | Fluxes to carcass scavengers |
| Food and feed | Fish production | Fluxes between prey and fish |
| | Hunted species production | Fluxes to hunted species |

^aAssociating NCP with specific trophic links is straightforward and a way to determine the amount of energy necessary for the ecosystem to sustain the contribution from nature. The table illustrates the associations between flux-related NCP and trophic links in ecological networks, which represent an estimate of the potential supply of these flux-related NOP.

^bThe categories of NCP shown were extracted from [53].

statistical modeling using biophysical (e.g., land cover, soil properties, or climate [12]), social or species-based (e.g., [13]) data [14]. In this way, most NCP derived from biophysical processes (e.g., carbon storage or prevention of soil erosion) and anthropogenic assets can be assessed and quantified, whereas flux-related NCP (e.g., pest regulation or fish production, but see Table 1 for more examples), which depend on the response of communities to different ecological drivers and the complex set of retroactions occurring because of species interactions, are not adequately captured and remain uncertain [9]. Here, we provide an integrative framework based on energy fluxes to upscale the estimation of ecosystem functions to large geographical scales and access the ecological supply of flux-related NCP [15], which represents the potential capacity of ecosystems to provide these NCP [16]. The approach we propose combines biodiversity data and species interactions into predictive models (Box 1 and Figure 1) to upscale energy fluxes for continental or global analyses. These models also offer the possibility to integrate future predictions from biodiversity scenarios, enabling forecasting of the future of ecosystem functions and flux-related NCP. Importantly, we emphasize that this framework does not incorporate NCP demand or the role of humans in the co-production of NCP. Appropriate transformation of potential capacity into realized supply, needed for decision and action, would require further work and could be a rewarding research area.

The biodiversity–ecosystem functions–NCP relationship: lessons from local scales

Biodiversity has a central role in regulating the fluxes of energy and matter that determine ecosystem functions and, ultimately, flux related-NCP [17]. At the local scale, calculation of energy fluxes allows for improved estimations of the effect of community structure [18] and environmental conditions [19,20] on multiple ecosystem functions simultaneously (multifunctionality). Therefore, it is often seen as a way to mechanistically study the interplay between biodiversity and ecosystem functioning, while taking a holistic approach that integrates the complexity of communities [2]. Similar types of question can be addressed when fluxes are associated with NCP. For example,

⁵Biology Department, McGill University, 1205 Docteur Penfield, Montréal, QC, H3A 1B1, Canada

*Correspondence:
ana_carolina.antunes@idiv.de
(A.C. Antunes).

the sum of energy fluxes associated with a fish species quantifies its biomass production, which can be used to estimate food provisioning from that species [7]. Similarly, quantifying the fluxes between an agricultural pest species and its predators provides an estimate of predation pressure on the pest species, which is a proxy for the strength of pest control at the moment the biodiversity data were sampled. Furthermore, this approach enables the incorporation of factors such as the sensitivity of food webs to disturbances (network stability [19]) and limitations on the transfer of biomass within trophic levels, which have a massive influence on the functioning of ecosystems and should be considered when predicting scenarios for flux-related NCP [21]. Typically, this use of energy fluxes to quantify ecosystem functions is tailored to estimate energy fluxes only at small spatial scales, usually for areas where experiments or individual measurements (e.g., species abundance or body masses) can be performed. Moreover, this framework relies on a set of ecological variables that are often accessible to ecologists locally: the list of occurring species, species biomasses, and body masses, and the set of trophic interactions between the taxa of the focal community. However, for regional or continental scales, these input data cannot be directly sampled, which hinders the application of this energy-flux framework to predicting ecosystem functions at macroecological scales.

Scaling up local estimations of ecosystem functions: biodiversity models as valuable tools

To evaluate energy fluxes and associate them with ecosystem functions and flux-related NCP at large spatial scales, challenges related to data acquisition must be overcome (**Box 1**), namely the low availability of data on species abundance and the identification and establishment of relevant **trophic links**. Despite significant gaps in biodiversity knowledge (e.g., for many tropical regions), significant progress has been made in predicting current and future species ranges and distributions [22]. These biodiversity models (referred to here as any model that predicts biodiversity data, such as abundance, interactions, and distribution) can fill in gaps in biodiversity data, providing a comprehensive representation of biodiversity, and their predictive capabilities (including species

Box 1. General workflow

- Step 1: Obtain the **metaweb** with potential species interactions.
- Step 2: Obtain species distributions for the study area.
- Step 3: Predict species density for each grid cell of the region of interest.
- Step 4: Obtain the local ecological network by subsetting the metaweb based on estimated species occurrences.
- Step 5: Calculate energy flux across the ecological network using species metabolic rates.
- Step 6: Associate fluxes of energy and/or species densities to NCP.

In general, local network topologies are obtained by subsetting the species list and interactions that occur within the region of interest (i.e., the metaweb). For the species list, different sources are available and can be used (e.g., IUCN[®] or GBIF[®]). The metawebs can be obtained directly from primary sources (e.g., TETRAEU [54]) or by extracting from aggregated databases (e.g., GLOBI [28]) the interactions for the taxonomic groups and the region of interest (Step 1). To subset the metaweb, local species occurrences need to be estimated from their large-scale distributions. Geographical limits based on expert opinion can be used to achieve this, possibly combined with species distribution models using occurrence data to further improve accuracy (Step 2). To calculate energy fluxes and, hence, evaluate NCP, it is necessary to build predictive models for species abundance to obtain local estimates of species biomasses. Data such as species biomasses and distributions can be derived at macroecological scales only through modeling. This is particularly relevant for species biomass, which can be predicted using species body mass and environmental conditions [36,37] (Step 3). Local networks are assigned by combining the metaweb of species interactions with the occurrence of species on the grid cell (Step 4). Fluxes throughout the network are calculated based on species metabolic rates (using allometric regressions that also incorporate temperature) and species biomasses arising from environmental conditions. Fluxes of energy can be calculated for single species or an entire trophic level (e.g., herbivores or species feeding on specific prey), depending on the NCP of interest (Step 5). The NCP to be evaluated should be associated with an individual flux of energy or summed network fluxes. By summing fluxes of energy across the grid cells, we can evaluate NCP across large spatial scales (Step 6). A workflow example on how to apply these steps is presented in the supplemental information online, associating the trophic control exerted by a natural predator on a crop pest species (**Figure 1**).

Glossary

Abundance models: predictive models to estimate the population abundance of species. Mostly based on species body mass, such models can also include species biological traits and environmental conditions.

Ecosystem functions: biological, chemical, and physical processes operating in an ecosystem that contribute to its stability and resilience (e.g., herbivory or productivity).

Flux-related NCP: set of NCP specifically derived from energy fluxes within species interactions (see **Table 1** in the main text for examples).

Food web models: characterize trophic interactions within an ecosystem to quantify energy fluxes between the different ecological groups.

Interaction models: use species traits (e.g., body mass or diet) and abiotic variables to predict the existence of interactions between species.

Metabolic rate: energy expended by an organism over a given period of time.

Metaweb: ecological network containing all the species that occur within the study area and all of their potential interactions. The elaboration of the network is usually based on species interactions previously described in the literature based on expert knowledge or field guides.

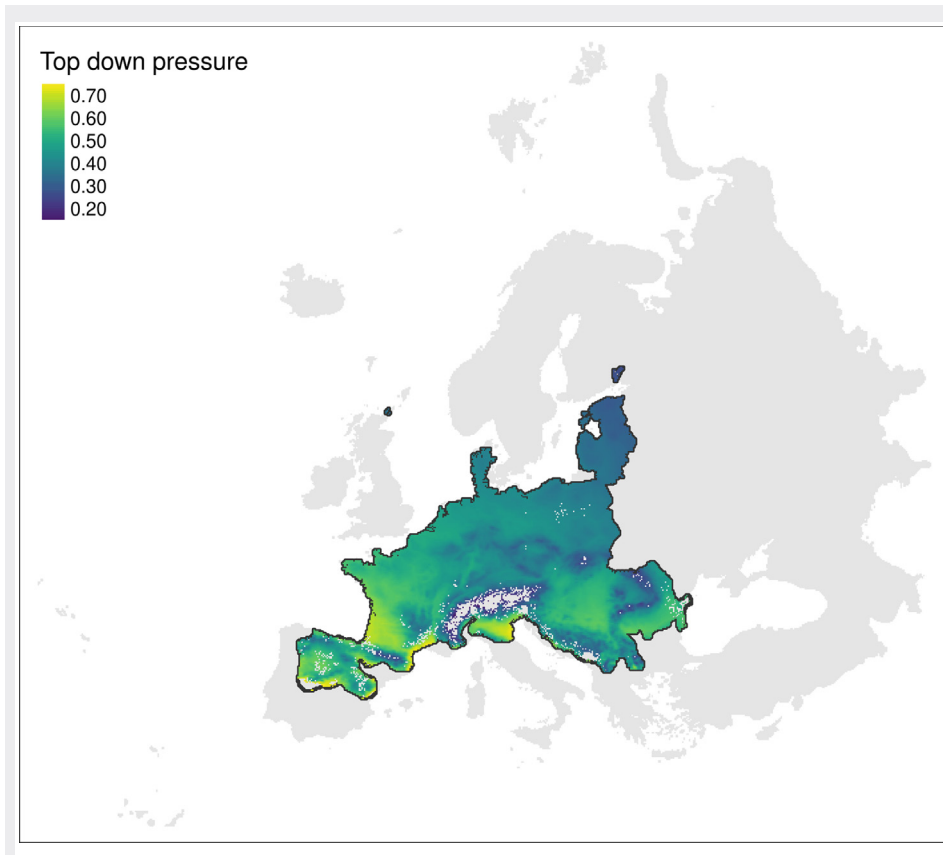
Nature's contributions to people (NCP)

(NCP): all the positive and negative influences of Nature on people's quality of life. There are 18 categories of NCP used in Intergovernmental Science-Policy Platform on Biodiversity and Ecosystem Services (IPBES) assessment.

Network topology: structure of a network that connects links and nodes. In ecology, species usually represent the nodes, which are connected through the links (e.g., energy links).

Species distribution models: predict or infer species distribution patterns across spatial scales, accounting for biotic (e.g., species interactions) and abiotic (e.g., environmental) factors.

Trophic link: feeding interactions between species in an ecological network.

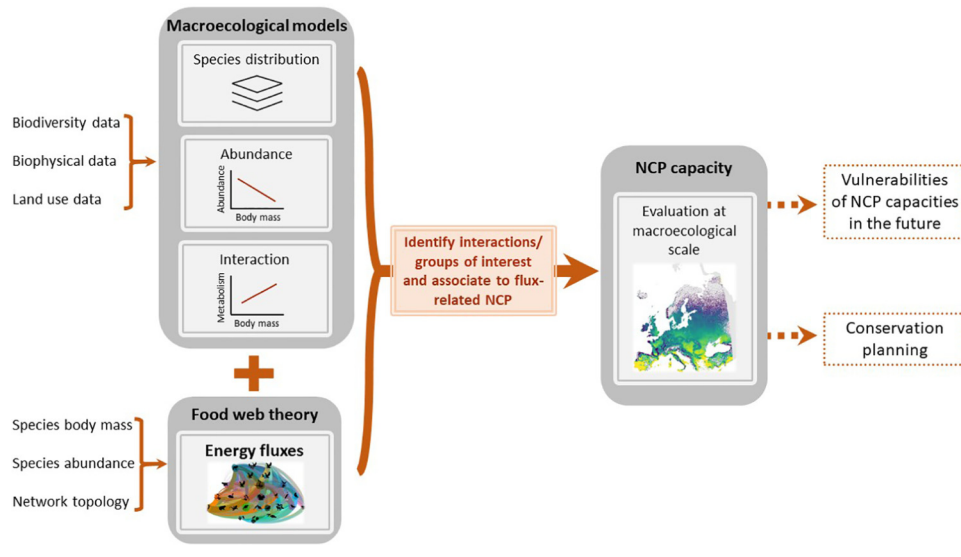


Trends In Ecology & Evolution

Figure I. Contribution of vertebrate species to the control of an agricultural pest (common vole, *Microtus arvalis*) mapped across the European continent. Map of the top-down pressure (associated with pest control) on *M. arvalis*, a rodent pest of agricultural fields across Europe (see also the supplemental information online). The lighter the color, the greater the top-down pressure. We emphasize that this result is intended to clarify how the framework can be applied to empirical data, and should not be used in further analysis or decisions.

occurrence, abundance, traits, and interactions) at regional, continental, and global scales are becoming more precise [22]. Three types of biodiversity model are needed to scale up local estimations of ecosystem functions through fluxes: **species distribution models**, **abundance models**, and **interaction models**.

Distribution (predicting species occurrence) and abundance (predicting species abundance) models generate predictions in plots, communities, or grid cells as a function of a set of environmental covariates. Environmental conditions exhibit considerable variation across an area, impacting physiological processes and, consequently, biodiversity patterns (e.g., distribution and abundance). Biodiversity models can account for this variation depending on their application (e.g., spatial scale or environmental variables used) and on the availability of data for the area [23]. The data sources used are also vital, and their availability will vary according to the location of the study area [24]. Therefore, environmental data should be carefully considered when predicting biodiversity patterns. These predictions can be extrapolated across space (e.g., to regions outside the extent of the original biodiversity data) or time (e.g., projected for future climate or



Trends In Ecology & Evolution

Figure 1. How biodiversity models and food web tools can be integrated to access the provision of flux-related Nature's contributions to people (NCP) at macroecological scales. Macroecological models and food web theory tools use different input data. The integration of these approaches allows the evaluation of ecosystem functions at large spatial scales. Through the identification of relevant taxa or interactions between species, we associate ecosystem functions with the potential supply of flux-related NCP.

land-use scenarios). Interaction models that predict the interactions between species, essential data for building the **network topologies** across space, are traditionally based on traits such as body mass [25], and recently started to incorporate abiotic variables [26,27]. Species interaction data can also be retrieved from global databases (e.g., GlobI [28] or GATEWAv.1.0 for trophic interactions [29]) containing information on various ecosystems and interaction types. While these databases may not document all the potential interactions of any given species, they provide a first and easily accessible source of data. Finally, algorithmic methods can reconstruct the missing parts of a network as soon as a reasonable amount of links are primarily identified [30–32]. A detailed protocol to infer species links for terrestrial ecosystems can be found in [33]. Together, these biodiversity models provide the information needed to calculate fluxes and, therefore, allow us to integrate biotic (e.g., species interactions and distributions) and abiotic (e.g., temperature, land use type, and resource availability) factors into a spatially explicit assessment of ecosystem functions. Moreover, we can also apply this framework across different time periods to assess, for example, ecosystem functions and predict future scenarios of flux-related NCP under different climatic and land-use conditions.

This incorporation of community information in the estimation of flux-related NCP comes at the cost of a more complex approach relying on different models, each based on a set of parameters suffering two limitations. First, each model is associated with a level of uncertainty that can percolate through the other models until the final predicted fluxes. However, it is possible to estimate this effect on final predictions through a bootstrapping approach (Box 2), which can also be used as a sensitivity analysis to test the importance of any parameter or process. Second, there is a bias in availability (toward low-latitude regions and vertebrate species, especially birds) and quality of biodiversity data [24] to inform the ecological models regarding the true species distributions. For example, the absence of information regarding species distributions constrains the effective utilization of species distribution modeling (SDM). To address this limitation, it is possible to combine

Box 2. Model uncertainty and validation

The accuracy of the flux estimations directly relates to the precision of the estimated parameters and the performance of the model used. A potential way to account for such uncertainty is through a bootstrapping approach, which can be used to generate a distribution of energy fluxes, rather than a single value, for each link of a local food web, thus describing the whole uncertainty due to modeling choices. By repeating the sampling and evaluating the estimated flux each time, we can obtain a distribution of flux for each trophic link of the food web and, therefore, an average prediction and associated uncertainty.

For species distribution models, different approaches exist to propagate uncertainty and enforce decisions [55]. One possibility is to associate species with a probability of occurrence based on the output of distribution models and to draw random realizations of species occurrences from a Bernoulli process. The level of uncertainty can then be quantified by evaluating the consensus among several distribution models. For instance, considering a species to occur only when there is agreement among all models will result in a more restrictive scenario compared with evaluating species occurrence based on a majority consensus. Estimations of species abundances usually rely on quantitative models based on statistical regression [35–37], from which it is possible to obtain, for each species, a probabilistic error function that can be used to sample a predicted abundance. Finally, occurrences of trophic links can be weighted using a probability of realization by quantifying species trophic niches [25,31] and then sampled using a Bernoulli process.

To validate our framework, one option is to compare the predictions obtained for an ecosystem function or NCP to what is measured in a few local sites, therefore estimating how good the model is at predicting: (i) the values of the specific function considered; and/or (ii) the trends observed in the values recorded at the different locations. Moreover, these confrontations between predictions and data can also be used to refine the hypotheses from the different models. Another option is to compare the predictions from our approach to other available modeling approaches at large spatial scales, whenever possible. This could be the case for not only well-studied or economically important flux-related NCP, but also new approaches that are continuously being developed for other NCP predictions. These comparisons can also help evaluate the importance of community composition and structure on the supply of flux-related NCP.

multiple models and data sources to increase model robustness or to incorporate expert knowledge and field observations to validate and refine model predictions. Furthermore, the approach upscales the evaluation of ecosystem functions and, therefore, quantifies the potential supply of flux-related NCP, which describes the capacity of the system to provide such contributions. The realized supply of flux-related NCP is not incorporated into this approach and would require further work, which could be a rewarding future research area.

The potential to integrate biodiversity models and energy fluxes

Large-scale studies assessing flux-related NCP still lack precision, especially when compared with the advances in evaluating biodiversity data at the same scale. By combining biodiversity information with energy fluxes, we expand our ability to predict flux-related NCP for areas where data are sparse or limited. Given that our framework incorporates different biodiversity models independently from each other, each step can be independently tested and validated. Therefore, the quality of final predictions can be tested in areas where data are available. As an example, abundance measurements, needed to evaluate the flux of energy between species, are usually rare and sparse [34], but trait-based biodiversity models are being developed to estimate average population abundances [35–37] and can account for climatic and biophysical factors. These abiotic parameters are also those used as inputs for species distribution models, making their integration consistent. In our workflow example (see the supplemental information online), we focus on trophic links, but similar workflows can be developed for NCP resulting from nontrophic interactions (Table 1). This approach can be implemented starting from a local grid cell (local ecological network), up to regional and continental scales. Moreover, the explicit consideration of food webs allows us to consider more finely how changes in community structures (e.g., distributions of species, their abundances, and **metabolic rates** across trophic levels) will affect ecosystem functions and flux-related NCP.

Our approach also creates a bridge to the large set of theoretical methods [38–41] offered by food web ecology, which can be incorporated into the approach to further test the effect of various perturbations. As an example, it is possible to estimate how communities would respond to disturbances

by calculating the resilience of the community based on the fluxes [19] (i.e., how the community will recover from a disturbance) or to assess the robustness of the estimated functions to species extinctions [39]. In the future, the approach could also be used to determine areas with a critical role in NCP supply and to identify key species supporting communities [7,41]. The loss of key species can trigger secondary extinctions, critically affecting not only the ecosystem functioning, but also the robustness of the flux-related NCP provided [40]. However, we emphasize that, before any use for conservation or decision-making purposes, the approach should be properly validated (Box 2).

Opportunities for future scenarios

Over the past 50 years, most NCP have declined globally as a consequence of climate and land-use alterations [42]. Although different future scenarios for climate and land-use change are used to predict NCP [43], flux-related NCP are usually overlooked. Our framework combines a modular approach that allows the integration of different elements related to global change scenarios that will affect differently the outputs of the models used. For instance, land use and increasing temperatures not only consistently impact species distributions [44] and local abundances of species [45], but also directly impact energy fluxes [19], ecological network structure, and trophic interactions [46,47]. Simultaneously, land-use change drastically impacts ecosystems through fragmentation processes, decreasing soil quality and increasing the risk of erosion, leading to biodiversity loss and causing a general decline in the abundance, diversity, and health of species and ecosystems [48,49]. Together, land use and climate change are thus likely to be key drivers of the variety, quantity, and spatial distribution of flux-related NCP through time [50].

Concluding remarks

Over the past decades, different methods have been developed to map the provisioning of NCP. Georeferenced metrics and geographic information system (GIS)-based approaches are the most commonly used and can efficiently account for spatiotemporal patterns and processes when quantifying NCP supply [51,52]. In contrast to other methods, our approach accounts for both biotic (e.g., species presence and interactions) and abiotic (e.g., environmental drivers) factors to upscale ecosystem function estimations and quantify the potential supply of flux-related NCP. In a broader context, this framework can be used to disentangle the impacts of environmental drivers (e.g., climate and land-use change) and community-level processes arising from trophic interactions on ecosystem functions and the supply of flux-related NCP at regional and continental scales. Thus, we show how this integrative approach opens new avenues to address unresolved questions (see [Outstanding questions](#)), and to improve our capacity to predict future changes in the supply of these NCP in the context of global change.

Acknowledgments

We acknowledge funding by the ERA-Net BiodivERsA - Belmont Forum call (project FutureWeb) and the Deutsche Forschungsgemeinschaft (DFG, German Research Foundation), project no. BR 2315/22-1. L.M.J.O.C. and W.T. also acknowledge support from the Horizon Europe NaturaConnect project (No. 101060429).

Declaration of interests

None declared by authors.

Resources

- ⁱwww.iucnredlist.org
- ⁱⁱwww.gbif.org

Supplemental information

Supplemental information to this article can be found online at <https://doi.org/10.1016/j.tree.2024.01.004>.

Outstanding questions

How can we expect ecosystem functions, such as productivity or herbivory, to be impacted in future scenarios of climate and land-use change within different parts of the world?

Are we overlooking the provision of NCP because we have not properly considered community processes in our assessment?

What are the consequences of diversity loss or gain to different NCP provisions at large spatial scales?

How do cascading effects on energy fluxes across ecological networks impact the supply of NCP?

How can we best integrate community processes and NCP capacity into conservation plans?

What are the similarities and/or differences between the output of this approach and others that do not consider community effects when estimating similar flux-related NCP (e.g., pest regulation or pollination)?

References

1. Cardinale *et al.* (2006) Effects of biodiversity on the functioning of trophic groups and ecosystems. *Nature* 443, 989–992
2. Barnes, A.D. *et al.* (2018) Energy flux: the link between multitrophic biodiversity and ecosystem functioning. *Trends Ecol. Evol.* 33, 186–197
3. Eisenhauer, N. *et al.* (2019) A multitrophic perspective on biodiversity–ecosystem functioning research. *Adv. Ecol. Res.* 61, 1–54
4. Jassey, V.E.J. *et al.* (2023) Food web structure and energy flux dynamics, but not taxonomic richness, influence microbial ecosystem functions in a *Sphagnum*-dominated peatland. *Eur. J. Soil Biol.* 118, 103532
5. Möllmann, C. *et al.* (2021) Tipping point realized in cod fishery. *Sci. Rep.* 11, 14259
6. Kortsch, S. *et al.* (2021) Disentangling temporal food web dynamics facilitates understanding of ecosystem functioning. *J. Anim. Ecol.* 90, 1205–1216
7. Nogues, Q. *et al.* (2023) The usefulness of food web models in the ecosystem services framework: quantifying, mapping, and linking services supply. *Ecosyst. Serv.* 63, 101550
8. Rey, P.-L. *et al.* (2022) *Mapping Linkages between Biodiversity and Nature's Contributions to People: A ValPar.CH perspective*, ValPar.CH
9. Ceau u, S. *et al.* (2021) Ecosystem service mapping needs to capture more effectively the biodiversity important for service supply. *Ecosyst. Serv.* 48, 101259
10. Harrison, P.A. *et al.* (2014) Linkages between biodiversity attributes and ecosystem services: a systematic review. *Ecosyst. Serv.* 9, 191–203
11. Ricketts, T.H. *et al.* (2016) Disaggregating the evidence linking biodiversity and ecosystem services. *Nat. Commun.* 7, 13106
12. Verhagen, W. *et al.* (2017) Use of demand for and spatial flow of ecosystem services to identify priority areas. *Conserv. Biol.* 31, 860–871
13. Luck, G.W. *et al.* (2009) Quantifying the contribution of organisms to the provision of ecosystem services. *Bioscience* 59, 223–235
14. Brauman, K.A. *et al.* (2019) Status and trends - Nature's contributions to people (NCP). In *Global Assessment Report of the Intergovernmental Science-Policy Platform on Biodiversity and Ecosystem Services* (Briand, E.S. *et al.*, eds), pp. 76, IPBES
15. Hummel, C. *et al.* (2019) Protected area management: fusion and confusion with the ecosystem services approach. *Sci. Total Environ.* 651, 2432–2443
16. Balvanera, P. *et al.* (2022) Essential ecosystem service variables for monitoring progress towards sustainability. *Curr. Opin. Environ. Sustain.* 54, 101152
17. Thompson, P.L. and Gonzalez, A. (2016) Ecosystem multifunctionality in metacommunities. *Ecology* 97, 2867–2879
18. Jochum, M. and Eisenhauer, N. (2022) Out of the dark: using energy flux to connect above- and belowground communities and ecosystem functioning. *Eur. J. Soil Sci.* 73, e13154
19. Schwarz, B. *et al.* (2017) Warming alters energetic structure and function but not resilience of soil food webs. *Nat. Clim. Chang.* 7, 895–900
20. Kordas, R.L. *et al.* (2022) Metabolic plasticity can amplify ecosystem responses to global warming. *Nat. Commun.* 13, 2161
21. Hines, J. *et al.* (2015) Towards an integration of biodiversity–ecosystem functioning and food web theory to evaluate relationships between multiple ecosystem services. *Adv. Ecol. Res.* 53, 161–199
22. Pollock, L.J. *et al.* (2020) Protecting biodiversity (in all its complexity): new models and methods. *Trends Ecol. Evol.* 35, 1119–1128
23. Randin, C.F. *et al.* (2020) Monitoring biodiversity in the Anthropocene using remote sensing in species distribution models. *Remote Sens. Environ.* 239, 111626
24. Hughes, A.C. *et al.* (2021) Sampling biases shape our view of the natural world. *Ecography* 44, 1259–1269
25. Gravel, D. *et al.* (2013) Inferring food web structure from predator-prey body size relationships. *Methods Ecol. Evol.* 4, 1083–1090
26. Li, J. *et al.* (2023) A size-constrained feeding-niche model distinguishes predation patterns between aquatic and terrestrial food webs. *Ecol. Lett.* 26, 76–86
27. Petchey, O.L. *et al.* (2008) Size, foraging, and food web structure. *Proc. Natl. Acad. Sci. U. S. A.* 105, 4191–4196
28. Poelen, J.H. *et al.* (2014) Global biotic interactions: an open infrastructure to share and analyze species-interaction datasets. *Ecol. Inform.* 24, 148–159
29. Brose, U. *et al.* (2019) Predator traits determine food-web architecture across ecosystems. *Nat. Ecol. Evol.* 3, 919–927
30. Caron, D. *et al.* (2022) Addressing the Eltonian shortfall with trait-based interaction models. *Ecol. Lett.* 25, 889–899
31. Rohr, R.P. *et al.* (2010) Modeling food webs: exploring unexplained structure using latent traits. *Am. Nat.* 176, 170–177
32. Williams, R.J. *et al.* (2010) The probabilistic niche model reveals the niche structure and role of body size in a complex food web. *PLoS ONE* 5, e12092
33. Hines, J. *et al.* (2019) A meta food web for invertebrate species collected in a European grassland. *Ecology* 100, 2679
34. Santini, L. *et al.* (2018) TetraDENSITY: a database of population density estimates in terrestrial vertebrates. *Glob. Ecol. Biogeogr.* 27, 787–791
35. Santini, L. *et al.* (2022) Population density estimates for terrestrial mammal species. *Glob. Ecol. Biogeogr.* 31, 978–994
36. Antunes, A.C. *et al.* (2023) Environmental drivers of local abundance–mass scaling in soil animal communities. *Oikos* 2023, e09735
37. Santini, L. *et al.* (2018) Global drivers of population density in terrestrial vertebrates. *Glob. Ecol. Biogeogr.* 27, 968–979
38. Gauzens, B. *et al.* (2019) Fluxweb: an R package to easily estimate energy fluxes in food webs. *Methods Ecol. Evol.* 10, 270–279
39. Srinivasan, U.T. *et al.* (2007) Response of complex food webs to realistic extinction sequences. *Ecology* 88, 671–682
40. Keyes, A.A. *et al.* (2021) An ecological network approach to predict ecosystem service vulnerability to species losses. *Nat. Commun.* 12, 1586
41. Allesina, S. and Pascual, M. (2009) Googling food webs: can an eigenvector measure species' importance for coextinctions? *PLoS Comput. Biol.* 5, e1000494
42. Brauman, K.A. *et al.* (2020) Global trends in nature's contributions to people. *Proc. Natl. Acad. Sci. U. S. A.* 117, 32799–32805
43. Stürck, J. *et al.* (2015) Spatio-temporal dynamics of regulating ecosystem services in Europe - the role of past and future land use change. *Appl. Geogr.* 63, 121–135
44. Newbold, T. *et al.* (2019) Climate and land-use change homogenise terrestrial biodiversity, with consequences for ecosystem functioning and human well-being. *Emerg. Top. Life Sci.* 3, 207–219
45. Bowler, D.E. *et al.* (2017) Cross-realm assessment of climate change impacts on species' abundance trends. *Nat. Ecol. Evol.* 1, 0067
46. Durant, J.M. *et al.* (2019) Contrasting effects of rising temperatures on trophic interactions in marine ecosystems. *Sci. Rep.* 9, 15213
47. Gilbert, J.P. (2019) Temperature directly and indirectly influences food web structure. *Sci. Rep.* 9, 5312
48. Davison, C.W. *et al.* (2021) Land-use change and biodiversity: challenges for assembling evidence on the greatest threat to nature. *Glob. Chang. Biol.* 27, 5414–5429
49. Hasan, S.S. *et al.* (2020) Impact of land use change on ecosystem services: a review. *Environ. Dev.* 34, 100527
50. Potts, S.G. *et al.* (2016) Safeguarding pollinators and their values to human well-being. *Nature* 540, 220–229
51. United Nations (2021) *System of Environmental-Economic Accounting—Ecosystem Accounting (SEEA EA)*, United Nations
52. Martin Belda, D. *et al.* (2022) LPJ-GUESS/LSMv1.0: a next-generation land surface model with high ecological realism. *Geosci. Model Dev.* 15, 6709–6745
53. Diaz, S. *et al.* (2018) Assessing nature's contributions to people. *Science* 359, 270–272
54. Maiorano, L. *et al.* (2020) TETRA-EU 1.0: a species-level trophic metaweb of European tetrapods. *Glob. Ecol. Biogeogr.* 29, 1452–1457
55. Araújo, M.B. and New, M. (2007) Ensemble forecasting of species distributions. *Trends Ecol. Evol.* 22, 42–47

Biotic filtering by species' interactions constrains food-web variability across spatial and abiotic gradients

Barbara Bauer^{1,2,3}  | Emilio Berti^{1,2}  | Remo Ryser^{1,2}  | Benoit Gauzens^{1,2}  | Myriam R. Hirt^{1,2}  | Benjamin Rosenbaum^{1,2}  | Christoph Digel⁴ | David Ott^{5,6} | Stefan Scheu^{7,8} | Ulrich Brose^{1,2} 

¹Institute of Ecology, Friedrich Schiller University Jena, Jena, Germany

²German Centre for Integrative Biodiversity Research (iDiv) Halle-Jena-Leipzig, Leipzig, Germany

³Zoological Institute and Museum & Institute for Botany and Landscape Ecology, University of Greifswald, Greifswald, Germany

⁴Umweltbundesamt, Dessau-Roßlau, Germany

⁵Institute of Landscape Ecology, University of Münster, Münster, Germany

⁶Centre for Biodiversity Monitoring, Zoological Research Museum Alexander Koenig, Bonn, Germany

⁷JFB Institute of Zoology and Anthropology, University of Göttingen, Göttingen, Germany

⁸Centre of Biodiversity and Sustainable Land Use, University of Göttingen, Göttingen, Germany

Correspondence

Remo Ryser, German Centre for Integrative Biodiversity Research (iDiv) Halle-Jena-Leipzig, Puschstr. 4, 04103 Leipzig, Germany.

Email: remo.ryser@idiv.de

Funding information

Deutsche Forschungsgemeinschaft, Grant/Award Number: FOR 2716, RTG 2010 and FZT 118

Editor: Kevin Lafferty

Abstract

Despite intensive research on species dissimilarity patterns across communities (i.e. β -diversity), we still know little about their implications for variation in food-web structures. Our analyses of 50 lake and 48 forest soil communities show that, while species dissimilarity depends on environmental and spatial gradients, these effects are only weakly propagated to the networks. Moreover, our results show that species and food-web dissimilarities are consistently correlated, but that much of the variation in food-web structure across spatial, environmental, and species gradients remains unexplained. Novel food-web assembly models demonstrate the importance of biotic filtering during community assembly by (1) the availability of resources and (2) limiting similarity in species' interactions to avoid strong niche overlap and thus competitive exclusion. This reveals a strong signature of biotic filtering processes during local community assembly, which constrains the variability in structural food-web patterns across local communities despite substantial turnover in species composition.

KEY WORDS

β -diversity, biodiversity, environmental distance, limiting similarity, meta-communities, meta-ecosystems, meta-food-webs, spatial distance

INTRODUCTION

Changes in species composition between sites (species dissimilarity or β -diversity) can be inflated by sampling error, but have been explained by neutral processes such

as random drift (i.e. random dispersal and establishment) or abiotic filtering (i.e. establishment depends on species niches' relative to abiotic factors; Hubbell, 2001; Tuomisto et al., 2003). Random drift implies that species dissimilarity is most strongly correlated with spatial distances between habitats, whereas abiotic filtering is indicated by a stronger

Barbara Bauer, Emilio Berti, and Remo Ryser shared first authorship.

This is an open access article under the terms of the Creative Commons Attribution-NonCommercial-NoDerivs License, which permits use and distribution in any medium, provided the original work is properly cited, the use is non-commercial and no modifications or adaptations are made.
 © 2022 The Authors. *Ecology Letters* published by John Wiley & Sons Ltd.

correlation with the dissimilarity of abiotic conditions (Tuomisto et al., 2003). Interestingly, both processes are random with respect to species interactions, which raises the question of whether the distribution of food-webs across local habitats can result from a simple random sampling of species from the regional pool. Understanding such spatial patterns in food-web structure is essential for drawing conclusions on community stability and ecosystem functioning (Barnes et al., 2018; Thompson et al., 2012).

Food-web structures vary along environmental and spatial gradients (Brose et al., 2004; Fricke & Svenning, 2020; Gauzens et al., 2020; Havens, 1993). As interactions depend strongly on species traits (Brose et al., 2019; Laigle et al., 2018), changes in species composition, and thus their traits, along these gradients could be the main driver of food-web dissimilarity. However, the relationship between species and food-web dissimilarities in space is not necessarily simple (Fründ, 2021; Ohlsson & Eklöf, 2020). For example, similar or different food-web structures across two habitats can arise from both a similar species composition (Figure 1a vs. b) and a different

species composition (Figure 1c vs. d). Of all possible species combinations under random sampling, many should be unlikely due to energetic and biological constraints. Hence, we hypothesise that the decay in similarity in food-web structures along spatial and environmental gradients should be weaker than the decay in similarity in species composition along the same gradients (H1).

In addition to the spatial processes (random drift and abiotic filtering) that drive species composition, we anticipate that biotic interactions with the species already present at the site (biotic filtering) contribute to patterns in food-web structure (Figure 1; Gravel et al., 2011; Massol et al., 2017). Ecological theory has identified two processes of how biotic interactions can drive local community assembly. First, any species needs a resource to successfully settle (Gravel et al., 2011), which causes community assembly to be initially dominated by generalist species that exploit a broad diet spectrum before specialists can invade (Piechnik et al., 2008). Second, the ecological niches of coexisting species should differ to avoid competitive exclusion (limiting-similarity theory, Abrams, 1996; MacArthur & Levins, 1967; Leibold, 1998),

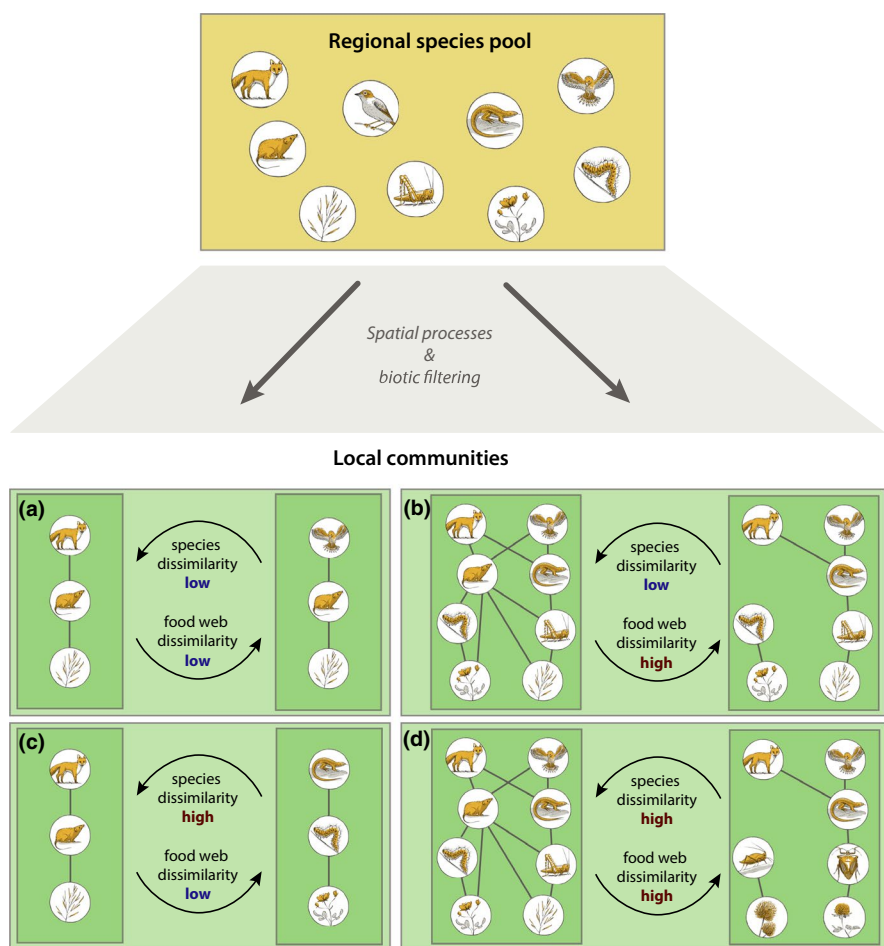


FIGURE 1 The potential relationships between species and food-web dissimilarity between pairs of local communities. Selection of species from the regional pool can be driven by spatial processes (e.g. dispersal, landscape structures) and biotic filtering (e.g. resource availability and limiting similarity) during community assembly. Variation in these processes or random events can result in pairs of local communities with species and food-web dissimilarities that are both low or high (a, d), in communities with low species dissimilarity but high food-web dissimilarity (b), or with high species dissimilarity but low food-web dissimilarity (c).

resulting in species' niche overlaps in local communities that are lower than expected by chance (Martins & Ferreira, 2020; Vergnon et al., 2013). Consequently, a low similarity of linkage patterns to resources and predators should increase the chances of successful establishment in a local community (limiting similarity). Therefore, we hypothesise that biotic filtering algorithms (resource and limiting-similarity filters) should improve the prediction of patterns in food-web dissimilarity across pairs of habitats in comparison to a random sampling of species from the regional pool (H2).

Here, we first compare the strength of the effects of spatial and environmental gradients on the variation in (1) species composition, and (2) inferred food-web structure using high-resolution empirical food-web data from forest soils and lakes (Digel et al., 2014; Havens, 1993). We then investigated if the empirically observed variability in potential food-web structure can be approximated by three simple models of food-web assembly that are based on (1) random selection of species from the regional pool without local filtering, or non-random selection based on species traits with (2) resource filtering, and (3) limiting-similarity filtering (see Figure 2 for filtering processes). Hence, we clarify the role of species composition and biotic filtering processes in driving the variability in food-web structures among local habitats.

MATERIAL AND METHODS

Empirical data

We analyse data from two empirical food-web datasets (Figure S3; Table S1). The first (soil dataset) includes 16 beech and coniferous forest sites within each of the three long-term research platforms Biodiversity Exploratories (Fischer et al., 2010). This yields 48 food-webs in total, each comprising 89 to 168 taxa (mostly species) of soil fauna and 730 to 3345 feeding interactions. Taxa comprise small basal microfauna, mesofauna and macrofauna. Environmental data for the 48 sites comprised C:N, C:P, and N:P ratios, soil pH and litter depth, mean soil moisture content and mean soil temperature data (Barnes et al., 2016; Klarner et al., 2014; Ott et al., 2014).

The second (lake dataset) comprises consistently sampled food-web data from 50 Adirondack lakes (Havens, 1993; Sutherland, 1989). The data includes 13 to 75 taxa (mostly species) of lake fauna and 17 to 571 feeding interactions, covering the complete pelagic food-web (piscivores, planktivores, zooplankton, and phytoplankton), except microbial components such as protozoans and bacteria. We used 14 environmental variables: maximum depth, surface area, volume, pH, acid-neutralising capacity, monomeric Al, dissolved organic carbon, total P, chlorophyll-a, spec conductance, SO_4^{2-} , NO_3^- , Ca^{2+} , and elevation. For simplicity, we refer to taxa in both datasets as species.

For both datasets, a binary matrix of feeding interactions was established among all taxa that were present

at any of the sites (hereafter: meta-food-web) based on literature data, as well as molecular methods, stable isotopes and feeding experiments in case of the soil dataset (Brose et al., 2019; Digel et al., 2014; Klarner et al., 2014; Laigle et al., 2018). We focused on binary food-webs as they indicate the presence and absence of species and links, whereas quantitative link data were not available. Individual food-webs for each forest or lake were established by extracting links of the species present at the site from the meta-food-web. Forest soil and lake food-webs were thus constructed assuming that any two species either interact or not across all locations (Digel et al., 2014; Havens, 1993). Hence, these food-webs are built under the assumptions that (1) species occur at sufficient abundance and temporal synchrony to realise potential interactions and (2) they do not adjust their diets in response to environmental conditions or co-occurring species (i.e. their competitors, predators or alternative resources). This excludes a possible effect that environmental conditions can modify some of these interactions (Tylianakis & Morris, 2017), which would result in additional interaction turnover. Dissimilarity in food-web structure thus arises from differences in species composition whereas other turnover in interactions is not included.

Calculation of distance matrices

To investigate species and food-web dissimilarities over spatial and environmental gradients we calculated two pairwise site distance (spatial, environmental) and dissimilarity (species and food-web) matrices for both datasets. We calculated *spatial distance* of sites as Great Circle Distance (the shortest distance between two points on the surface of a sphere instead of a straight line through the sphere's interior). To calculate *environmental distance* between sites, we performed a principal component analysis (PCA) for the two datasets separately using all variables and retained the principal components that explained cumulatively at least 70% of the total variance. We then used the remaining principal components to calculate the environmental distance as the Euclidean distance among sites. Three principal components were used for the soil dataset (variance explained = 73.3%) and four components were used for the lake dataset (variance explained = 71.4%).

Species dissimilarities were calculated as Jaccard dissimilarities of sites based on their species compositions (presence-absence). We included all taxonomic groups when computing the Jaccard dissimilarity, which is common in studies focusing on meta-communities (Grainger & Gilbert, 2016) and spatial ecosystem functioning (Menge et al., 2015).

We calculated *food-web dissimilarity* between sites in a similar way as for the environmental distance. As there is no single index that completely characterises the structure of complex food-webs (Delmas et al., 2019), we included several metrics, capturing structural

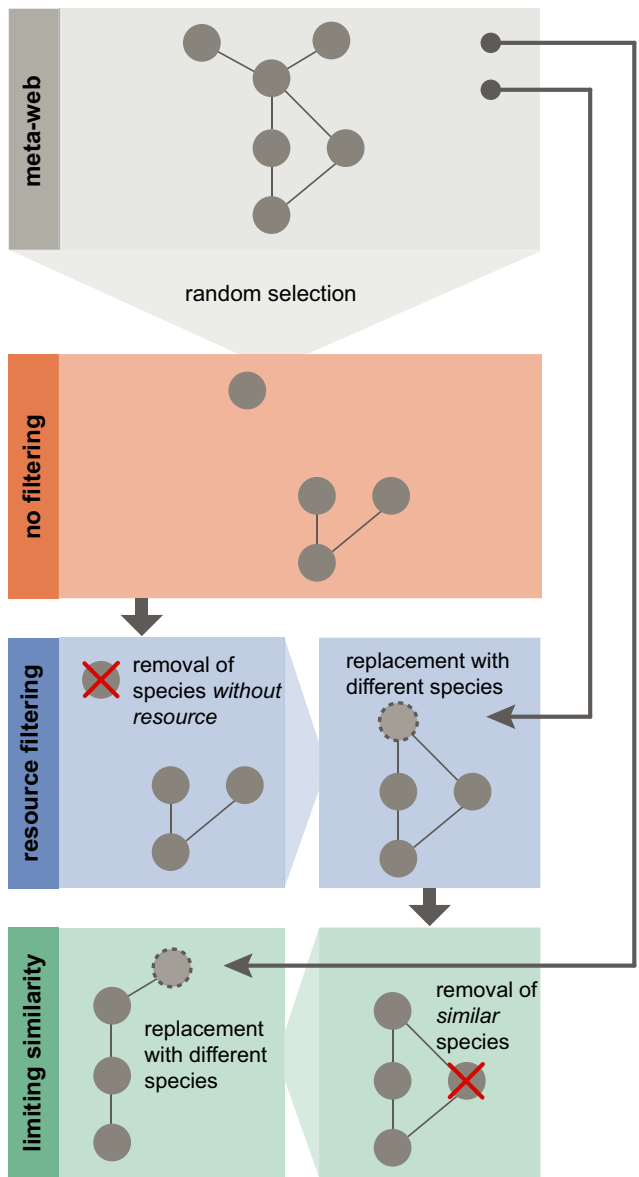


FIGURE 2 Conceptual representation of the simulations. For each meta-food-web and pairs of local sites, species were sampled at random until the two simulated food-webs had similar species richness and number of shared species as the empirical counterparts (no-filtering). We then imposed all species to be connected, directly or indirectly, to basal species, in order to persist in the local food-webs (resource filtering). Species that did not meet this condition were replaced by others sampled at random from the meta-web (long arrow) until connected food-webs were found. To examine a scenario where also trophic traits of species influence their probability of occurring in the local food-webs (limiting-similarity-filtering), we implemented an algorithm where species that have similar trophic niches were unlikely to co-exist and were substituted by others sampled at random from the meta-web (long arrow) subsequent to the resource-filtering process. In the context of this study, removal and replacement refer to the algorithm steps and not to ecological dynamics of food-webs

aspects along a continuum from the meso- to the whole-network scale, in order to quantify different aspects of the topology and composition of food-webs. Such descriptors can be classified into four types of metrics: (1)

structural indices, characterising the complexity of the whole network, included connectance (ratio of the number of realised to potential links; *Con*), clustering (*clust*), the average trophic similarity (*meanSim*), standard deviation of the normalised generality (*sdGen*), standard deviation of the normalised vulnerability (*sdVul*) and characteristic path length (*CPL*). (2) Trophic level indices, representing whole-network properties of the energy pathways from primary producers to consumers, included maximum, mean, and standard deviation of trophic levels (*maxTL*, *meanTL*, *sdTL*, respectively). (3) Fractions of functional groups comprised the number of basal (*frB*, those with no prey), intermediate (*frI*, those that have both predator and prey), top predator (*frT*, those that have no predators) and omnivorous (*frOmn*) species divided by the total number of species in the web. (4) Frequencies of motifs, illustrating meso-scale properties of the network, included intraguild predation (*fIGP*), apparent competition (*fAC*), trophic chain (*fTC*), and resource competition (*fRC*). We performed a PCA using all metrics for each dataset separately and retained the principal components that explained at least 70% of the total variance (Figure S4). We then used the remaining principal components to calculate food-web dissimilarity as the Euclidean distance among sites. Two principal components were used for both the soil (variance explained = 74.0%) and the lake datasets (variance explained = 72.2%).

Statistics on the relationships between distance metrics

In order to test our first hypothesis, we used a structural equation model (SEM; Figure 3) to determine the relative effect sizes (range-standardised path coefficients representing the relative importance of a predictor) for the soil and lake datasets. Soil and lake datasets were analysed separately. We employed a covariance-based global estimation using the R-package "lavaan" (Rosseel, 2012). SEM included paths representing potential causal association among variables, these being an influence of spatial distance on environmental distance and species dissimilarity, of environmental distance on species and food-web dissimilarity, and of species dissimilarity on food-web dissimilarity. To test if spatial distance directly influences food-web dissimilarity, we compared our SEM with the full model, including also the direct effect of spatial distance on food-web dissimilarity; if this direct effect was important, the two models would differ significantly. Importantly, although the turnover of species interactions does not vary across the environmental gradient in our datasets, this can still influence food-web structure by selecting species with specific trophic roles, e.g. consumers with high trophic levels. Thus, we also investigated the association between

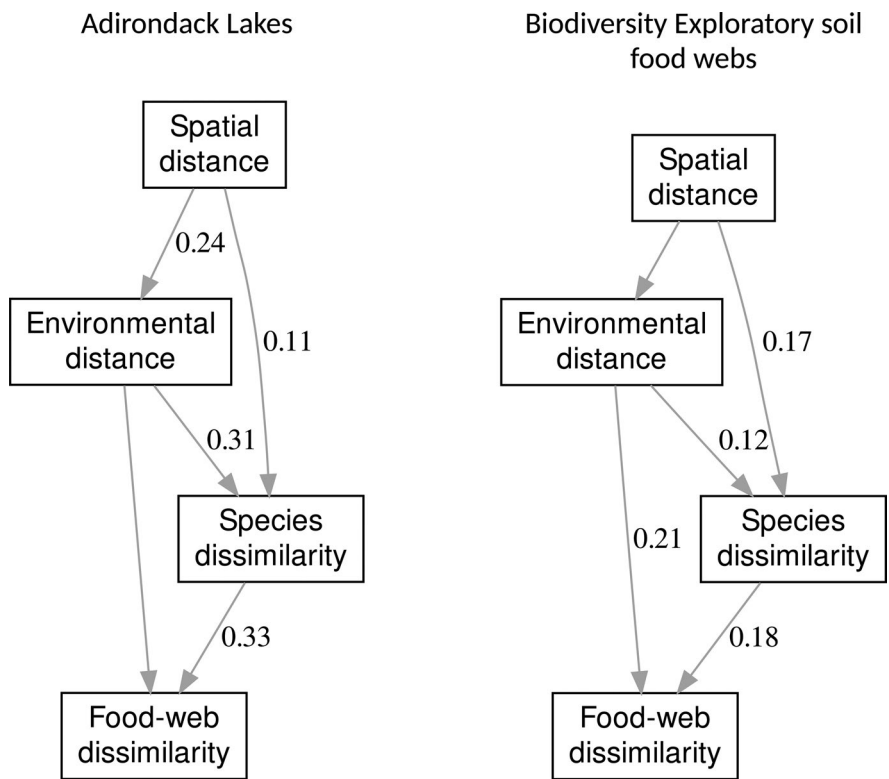


FIGURE 3 Structural equation models (SEM) for lakes (left, $n = 1213$, chi-squared test for goodness-of-fit: $\chi^2 = 0.141$, $df = 1$, $p = 0.707$) and soils (right, $n = 359$, $\chi^2 = 0.017$, $df = 1$, $p = 0.898$). Arrows represent SEM structure, annotations are standardised path coefficients and indicate each predictor's significant relative effect size. As we standardised variables from the two datasets jointly, coefficients are quantitatively comparable between lake and soil datasets. Arrows without annotation represent non-significant effects

environmental distance and food-web dissimilarity to account for such potential effects that are not captured by the community-level metric of species dissimilarity.

As soil food-webs were spatially clustered into three blocks (Figure S3), we considered pairwise comparisons only between food-webs within the same spatial block, removing all inter-block comparisons. This was necessary to avoid biases in our analysis due to differences among distant spatial blocks that were not caused by the ecological processes of interest. The spatial distance was log₁₀-transformed before analysis to improve the model fit and all variables were standardised separately for the soil and lake datasets. We then ran one SEM for the soil ($n = 359$) and one for the lake ($n = 1213$) dataset.

As pairwise comparisons may violate assumptions of non-independence when using the whole dataset, where a site appears more than once, we assessed whether this inflated type I error by performing a bootstrap sensitivity analysis (Supporting Information). This consisted of 100,000 SEMs evaluated using only a small random subset ($n = 48$ for soils, $n = 50$ for lakes) of the whole dataset and from which we obtained bootstrapped means and 95% confidence intervals for the path coefficients. We also conducted a separate simulation to evaluate the extent to which sampling error could drive some of the associations between communities and networks.

Simulations

We tested if dissimilarity between local food-webs assembled by simulations can replicate empirically observed dissimilarity, given the same amount of species dissimilarity. The assumptions used to construct simulated webs are that (1) there are no constraints imposed on local food-web structures (such as limits on maximum trophic levels); (2) local food-web structures solely emerge based on the trophic properties of species that are entering the site from the regional species pool; (3) these trophic properties do not influence the likelihood of a species being present at any given site. We then investigated if adding filtering processes for species to be able to enter or persist in the local food-webs creates a closer resemblance in simulated food-web dissimilarity to the empirical one. We examined two filtering processes: resource filtering, where species can enter the local food-web only if they have available resources, and limiting-similarity filtering, where trophic similarity of species influences their probability to establish in the local pools (Figure 2).

We explored the assembly processes for the two empirical meta-webs of the soil and lake datasets using three assembly algorithms: 'random', 'resource filtering', and 'limiting-similarity-filtering'. We iterated the following steps over all possible pairwise combinations

of sites within the two datasets. First, we calculated the number of species (S_1, S_2), number of shared species (S_{sh}) and the 17 food-web properties (as described above) for the empirical sites. For each food-web property i and site pair, we calculated the empirical food-web difference, $\Delta_{e,i}$ as the absolute value of their difference between the sites. We then considered a random assembly process by drawing random species from the meta-webs until we assembled a pair of local species pools with the same total number of species in each site (S_1, S_2) and number shared between them (S_{sh}). We constructed local food-web adjacency matrices by extracting rows and columns corresponding to local species from the model meta-web. We then calculated the 17 food-web properties of these model local webs as well as their difference, $\Delta_{m,i}$. Finally, we computed the deviation of the model difference ($\Delta_{m,i}$) from the empirical difference ($\Delta_{e,i}$) for each of the 17 food-web properties i , site pair (1128 for soils and 1225 for lakes) and model meta-webs. If a model web did not contain basal species, we omitted the calculation of trophic level indices. Each filtering algorithm was replicated 200 times per site pair, from which we calculated $\Delta_{m,i}$.

From these randomly assembled species pools, we imposed further constraints for species to (co)exist locally by adding resource filtering and limiting-similarity-filtering processes. The resource filtering imposed that all species were connected, directly or indirectly, to basal resources. The limiting-similarity-filtering simulated a

probabilistic process where species with similar trophic niches were unlikely to co-exist and were replaced by random species from the meta-web. In order to assure all species were connected within the community, limiting-similarity-filtering was always performed in combination with resource filtering. We made sure that local species pools after both resource and limiting-similarity filterings had the same values of species richness (S_1 and S_2) and species shared (S_{sh}) as the empirical counterparts; otherwise, local species pools were discarded. Details of the filtering processes can be found in Figure 2 and Supporting Information. We compared empirical and simulated food-webs by performing simple linear regression between species and food-web dissimilarities and obtaining the Cohen's d effect size of the slopes (Cohen, 2013). Effect sizes closer to the empirical ones indicate stronger support for the biotic filtering process involved in the simulation. All simulations and analyses were done in the R programming language (R Core Team, 2019).

RESULTS

In the lake dataset, spatial distance influenced environmental distance ($p < 0.05$, estimate = 0.239), indicating a spatial signature in environmental variables for this dataset (Figures 3 and 4a). However, in the soil dataset, this association was not significant ($p = 0.555$), indicating that environmental variables were not

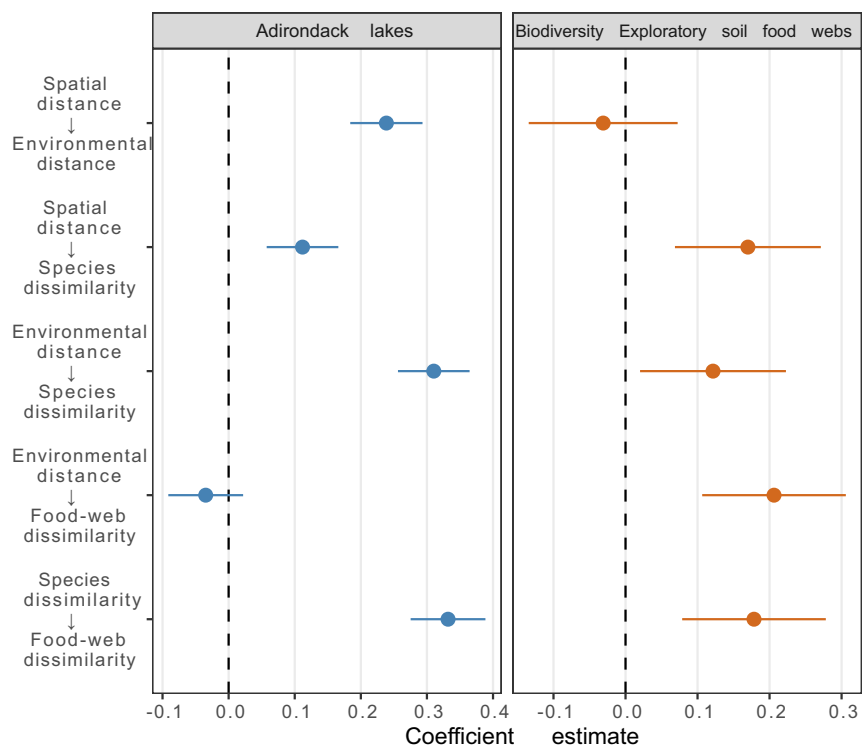


FIGURE 4 Coefficient estimates from structural equation models (SEM). Points show the coefficient estimates and lines the 95% confidence intervals. SEM coefficients that have confidence intervals crossing zero (dashed line) are not significant. Only direct path coefficients that are significant in at least one of the two datasets are displayed

spatially structured. Interestingly, the two community types exhibited different responses to spatial and environmental gradients (Table S2). While in the lake dataset environmental distance had a stronger effect on species dissimilarity (estimate = 0.310) than spatial distance (estimate = 0.112; Figure 4b,c), the opposite was true for the soil dataset, for which species dissimilarity depended more strongly on spatial distance (estimate = 0.170) than on environmental distance (estimate = 0.121). These results show that the lake communities were more strongly driven by abiotic filters, whereas the soil communities depended more strongly on a random spatial drift.

Our SEMs were not significantly different from the full models, i.e. including also a direct association between spatial distance and food-web dissimilarity, for both lake ($\chi^2_{df=1} = 0.141, p = 0.707$) and soil ($\chi^2_{df=1} = 0.017, p = 0.898$) datasets, indicating that in both datasets spatial distance did not influence food-web dissimilarity directly (Figure 4d). Environmental distance did not affect food-web dissimilarity in the lake dataset; in the soil dataset, however, this association was significant and positive ($p < 0.05$, estimate = 0.206), indicating that similar environments had more similar food-web structure. In both datasets, food-web dissimilarity was directly influenced by species dissimilarity ($p < 0.05$; Figure 4f), with this relationship being stronger in the lake (estimate = 0.332) than in the soil dataset (estimate = 0.178). Notably, the association between species dissimilarity and food-web dissimilarity had the highest partial path coefficients in the lake dataset, indicating that food-web structure was shaped more by species composition than by direct effects of spatial and environmental filters. On the other hand, in the soil dataset, the influence of species composition on food-web dissimilarity was comparable in magnitude to that of the environment. When comparing bootstrap path coefficients with results using the whole dataset we found that while the coefficients were consistent with the original pairwise analysis, many of the 95% confidence intervals (CL) for all bootstrapped coefficients overlapped with zero (Table S2), suggesting the associations among variables could not be distinguished from random variation. Only in the lake communities, our sensitivity analysis suggests positive relationships between (1) species dissimilarity and environmental distance, and (2) species dissimilarity and food-web dissimilarity. Combining together direct and indirect effects in these SEMs, the total amount of variation explained in food-web dissimilarity was only 10.4% for the lake and 8.3% for the soil dataset, highlighting that spatial and environmental gradients and species composition constrain food-web structure only weakly. Moreover, in a second sensitivity analysis we have also assessed the influence of potential sampling errors (false negatives) on species composition (i.e., missing species in the local samples). Our Monte-Carlo approach revealed that for a wide range of potential sampling errors, namely up until

50% of the species in pairs of local patches were erroneously omitted, we found that the slope of the relationship between food-web and species dissimilarities was not affected by such potential biases (Figures S1 and S2, comparing black estimates to solid lines). However, we also compared the slopes to a second set of sampling error simulations, in which we compared each community to itself along a gradient of imposing independent sampling error on both instances of this community. As our SEM estimates of the slopes fall within the confidence limits of these simulated sampling-error slopes, we cannot rule out that the limited food-web dissimilarity found in our empirical data is caused by sampling error. Taken together, these results are mostly consistent with our first hypothesis (H1) that the relationships between spatial or environmental distances with food-web dissimilarity are weaker than those with species dissimilarity. Only in the soil dataset, the influence of species dissimilarity on food-web dissimilarity was comparable to the effect of environmental distance (Figures 3 and 4). The confidence intervals of these two coefficient estimates overlap substantially (Figure 4), and we thus concluded that these two effects are similar in strength. As the direct influence of environmental distance on food-web dissimilarity in the soil dataset cannot be explained by interaction turnover, this implies that the environment shapes food-web structure by selecting a few species that have unique trophic roles in otherwise largely similar communities. Overall, our findings suggest that spatial and environmental distances affect community composition (which species are present in a given location), but only to a minor extent, if at all, food-web topology (the energetic structure describing how those co-occurring species are linked).

The low amount of variability explained in food-web dissimilarity by the SEM highlights that other processes might be important in shaping food-web structure. To understand what could be the source of this variability, we hypothesised that random spatial drift of species and biotic filtering processes by species interactions during community assembly should be responsible for dissimilarity patterns in food-web structure across gradients in community composition (H2). As a first step towards understanding which biotic filtering processes could have created the observed patterns in food-web dissimilarities, we compared the empirical food-web dissimilarity patterns with those arising from simulated random samples from the empirical meta-food-webs under (1) no-filtering, (2) resource filtering, or (3) limiting-similarity-filtering. By comparing simple regression effect sizes, we found that increases in food-web dissimilarity with species dissimilarity were roughly consistent between empirical and the three types of simulated communities for both datasets (Table S3). For instance, for the lake dataset, slope effect sizes were 0.384 using the empirical meta-web, 0.406 from simulations using random meta-webs with no-filtering, 0.294 using resource filtering, and

0.451 imposing also the limiting-similarity-filtering. For the soil dataset these were, 0.332, 0.173, 0.141, and 0.193, respectively. The higher discrepancy between empirical and simulated effect sizes for soil food-webs suggests more shallow slopes in the simulated compared to the empirical communities. However, the general pattern emerging across empirical and simulated communities is that all relationships exhibited comparably weak effect sizes (Table S3). In addition to these mean trends, we also compared the distribution of the empirical and model predictions' residual deviations from the empirical fitted linear model (Figure 5), which highlights how much of the observed variability in food-web structure for a given species dissimilarity value is explained by each model. The empirical relationships between food-web and species dissimilarity yield empirical distributions of residuals (black distributions in Figure 5). We calculated the deviation of each of the three simulated models' predictions on food-web dissimilarity from the empirical relationship, which yielded three residual distributions that can be benchmarked against the empirical distribution. These comparisons revealed for both lake and soil communities that across all food-web properties the limiting-similarity-filtering yielded residual distributions that are closest to the empirical distributions (Figure 5a,b, green vs. black). The resource filtering exhibited the strongest deviation from the empirical distributions, whereas the no-filtering model produced intermediate deviations (Figure 5a,b, blue and orange). Generally, the no-filtering and the resource-filtering models overestimated the right tail of the empirical distributions, which suggests that they predict communities with too high food-web dissimilarity for a given species dissimilarity. In contrast, the limiting-similarity model, while being closest to the empirical distributions, underestimated the right tail, which implies that the predicted food-web dissimilarity is too low. Despite these obvious deviations from the empirical patterns, our results suggest that the filtering processes are likely to contribute to community assembly.

These differences in overall food-web dissimilarity between empirical data and the simulated models also become apparent in specific food-web metrics (Figure 5c,f; Figure S6). We found that all three simulated models yielded quite accurate predictions of dissimilarity patterns in some properties. However, the no-filtering model predicted the mean trophic level best, whereas the two biotic filtering models yielded systematic over predictions (Figure 5c,d). This suggests that processes not accounted for by the biotic filtering models constrain the empirical trophic levels. Another striking difference is that the resource-filtering model provided the most accurate estimates of dissimilarity in connectance (Figure 5e,f), whereas both the limiting-similarity and the no-filtering models predicted food-web pairs that were more similar in connectance than found empirically. This hints at additional filtering processes that create more variance in the linkedness of the populations.

DISCUSSION

Our empirical analysis of variability in potential food-web structure across local lake and soil communities revealed systematic relationships with changes in their species composition. Our first hypothesis (H1), i.e. that spatial and environmental distances impose a weaker influence on food-web structure than on community composition, is supported by our results for the lake dataset and, at least partly, for the soil dataset, for which environmental distance had an effect on food-web structure comparable to that of species composition. As interaction turnover was not present in our datasets, the latter result can only be explained by the environment filtering, within largely similar communities, for a few species with unique trophic roles that strongly affect food-web structure. This direct effect of the environment on food-web structure for the soil dataset is, however, weaker than the direct effect of species composition, suggesting that the main driver structuring food-webs also is how communities assemble due to abiotic processes and random drift. In accordance with our second hypothesis (H2), we found that empirically observed cross-site differences in various types of food-web properties can be approximated by novel food-web assembly models, without assuming direct environmental or spatial effects generating food-web variability. In this sense, our food-web assembly models highlight the importance of species' interactions creating biotic filtering processes during local community assembly that constrain variability in food-webs across spatial and abiotic gradients.

Spatial and environmental distance may have exerted effects on species dissimilarity in the soil and lake communities, respectively. Processes that have spatially structured ecological communities have been inferred using multivariate methods to partition the effects of spatial distance and environmental dissimilarities among sites on the dissimilarities of their species distributions (Gilbert & Lechowicz, 2004; Lindström & Langenheder, 2012; Tuomisto et al., 2003; Viana & Chase, 2019). Our sensitivity analyses suggest that a significant portion of the β -diversity patterns may also be related to sampling error, and the associated levels of significance are affected by the statistically questionable replicated use of data from a single site in data on inter-site turnover, which violates the assumption of data-point independence. Additionally, substantial fractions of unexplained variation in species dissimilarity in these and our study may arise from sampling errors associated with variance in species abundances and movement rates (Brose & Martinez, 2004). Studies are just beginning to explore how the spatial scale of the analysis, habitat heterogeneity, dispersal rates, and regional pool size influence the outcome of such variance partitioning analyses (Leibold & Chase, 2018).

Compared to the large body of literature on understanding variability in species composition, insights

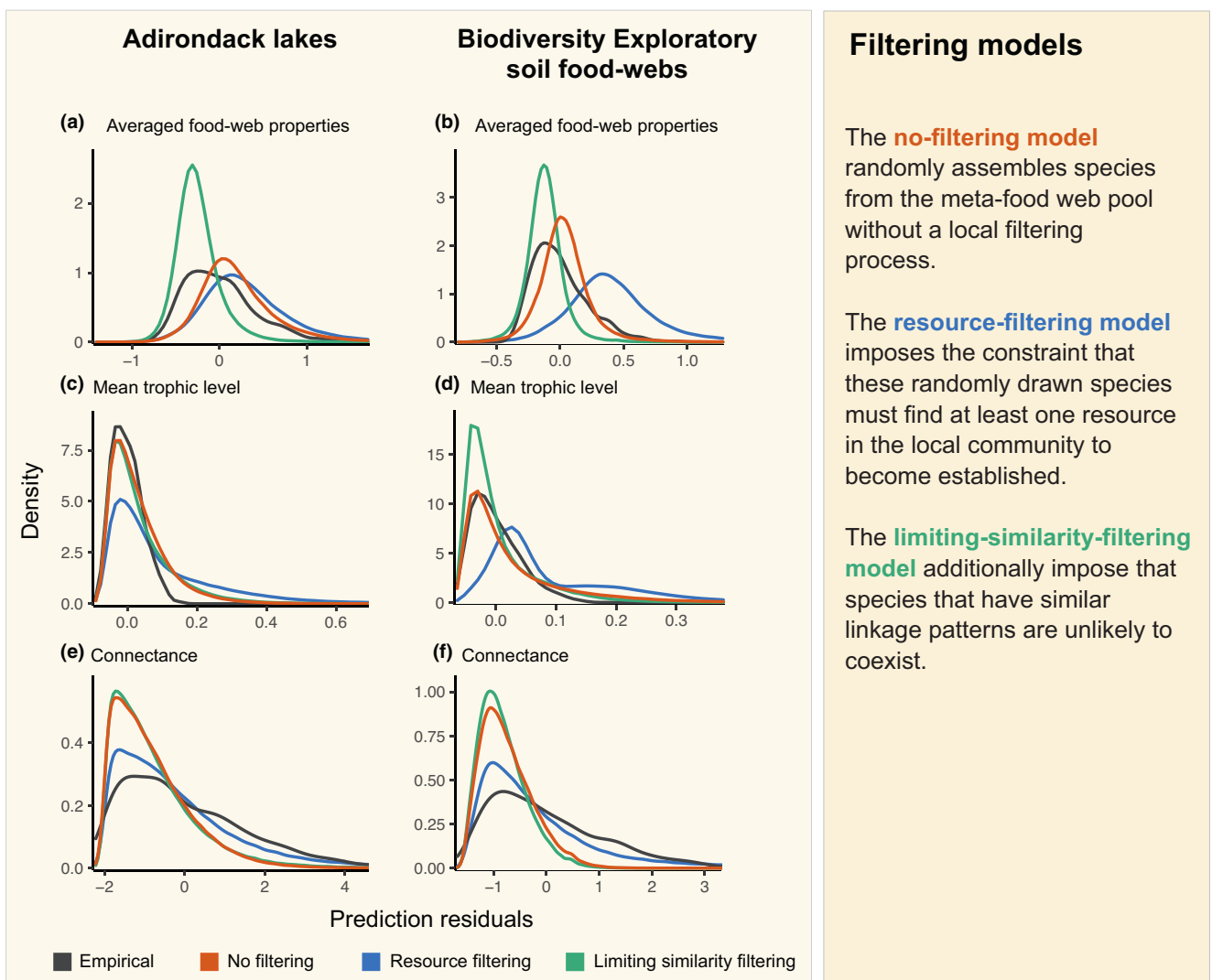


FIGURE 5 Overlayed distributions of predicted residuals depicting how similar the simulation results with different biotic filters (no-filtering—orange; resource filtering—blue; limiting-similarity-filtering—green) are compared to the distribution of residuals of the empirical data (black) for both ecosystems (a, c, e—Adirondack lakes; b, d, f—Biodiversity Exploratory soil food-webs). Empirical residuals were obtained from linear models with the scaled and centred species dissimilarity as the independent variable and the first scaled and centred and the averaged differences in food-web properties (a, b) or the individual scaled and centred difference of the food-web properties (c, d)—mean trophic level; e, f—connectance). The distributions of the residuals from the simulations were obtained as the difference between the model prediction and empirical prediction

into what ecological processes can be inferred from observed patterns of spatial variability in food-web structure are scarce (Brose et al., 2004; Galiana et al., 2018). Interestingly, our results reveal that changes in food-web structures across spatial and environmental gradients are limited in comparison to dissimilarities in species composition. Additionally, our sensitivity analyses indicate that this limited change in food-web structure cannot necessarily be separated from effects of potential sampling error in species composition. Overall, then, our results support the expectation by our first hypothesis (H1) that the topological structure of food-webs is quite conserved, even over large spatial distances and changing environmental conditions. This suggests that, instead of assuming simple dependencies of local

food-web topologies on species composition driven by abiotic conditions (Tylianakis & Morris, 2017; Tylianakis et al., 2018) or spatial processes (Brose et al., 2004; Fricke & Svenning, 2020), we also need to consider constraints by local biotic filtering processes during community assembly.

We have compared the empirical patterns in food-web dissimilarity to those generated by three food-web assembly models (no-filtering, resource filtering, and limiting-similarity-filtering), using the empirical meta-webs from the lake and soil datasets. The *no-filtering model* randomly assembles species from the meta-food-web pool without a local filtering process. The *resource-filtering model* imposes the constraint that these randomly drawn species must find at least one resource in the local community

Filtering models

The no-filtering model

randomly assembles species from the meta-food web pool without a local filtering process.

The resource-filtering model

imposes the constraint that these randomly drawn species must find at least one resource in the local community to become established.

The limiting-similarity-filtering model

additionally impose that species that have similar linkage patterns are unlikely to coexist.

to establish. The *limiting-similarity-filtering model* additionally imposes that species with similar linkage patterns are experiencing strong competition and are thus unlikely to co-exist (Martins & Ferreira, 2020; Vergnon et al., 2013). We found that these simple food-web assembly models could in general reproduce the magnitude of observed food-web differences and the weak scaling relationships with species dissimilarity across local communities. The limiting-similarity model performed best in predicting patterns in food-web dissimilarity across both datasets. This is particularly striking as the two community types are driven by very different processes. In the lake dataset, assembly is mainly driven by constraints of acidification (Sutherland, 1989) on species richness with associated turnover in linkage densities (Brose et al., 2004). In the soil dataset, environmental factors contributed little to drive the overall composition of communities compared to spatial patterns of species distribution. For both ecosystem types, abiotic filtering might exhibit stronger signatures in the food-web structures when accounting for environmental constraints on within-species traits, abundances, and thus realised interactions. Nevertheless, these results may be taken as a first, albeit preliminary, indication that the relative importance of biotic filtering processes in general and the limiting-similarity filtering, in particular, might be important across very different ecosystem types.

Meta-food-web theory does not provide clear hypotheses on how assembly processes should affect specific network properties. Here, we found that the success of simple food-web assembly models in predicting spatial patterns in overall food-web dissimilarity is also reflected in their consistently accurate predictions of some specific aspects of food-web topology. Nevertheless, we found strong deviations from their predictions from empirical patterns in other specific aspects of food-web topology. For example, indices related to trophic levels showed higher variation in model predictions than in empirical networks. This low variation observed in empirical food-webs is likely due to energetic constraints (e.g. the primary productivity of the local sites) that limit variation in the number and distribution of trophic levels in real food-webs. This result highlights the need to incorporate energetic constraints of primary productivity (Keva et al., 2021; Oksanen et al., 1981) and temperature (Binzer et al., 2016; Keva et al., 2021) on food-chain length and the number of trophic levels into filtering models for local food-web assembly.

Despite the success of the simple food-web assembly models in predicting some aspects of food-web dissimilarity across local communities, we see opportunities for their improvement. First, including energetic constraints (e.g. based on the site's primary productivity) on the maximum number of trophic levels that can be established may eliminate some inaccuracies in the predictions (see above). Second, all of these filtering models relate to the local linkage patterns of species, and filtering models that correspond to the overall network structure could

provide additional insights into food-web assembly. For instance, stability constraints on food-web complexity (Rall et al., 2008) could create a filter that influences the likelihood of persistence of generalists versus specialists. Third, food-web assembly could be modelled as a continuous process of local removals and invasions. In this sense, removal and invasion success could depend on species traits such as body mass, resource specificity, or trophic level, which can have secondary effects on the persistence of other species (Curtsdotter et al., 2011). Fourth, biological filtering could be combined with spatial processes by accounting for trait-dependent differences in species dispersal capacities (Hirt et al., 2018), especially if these differences are correlated with trophic traits (Hirt et al., 2020). Overall, combining filtering approaches that consider such dispersal limitation and abiotic filtering (Muñoz et al., 2018) with those that focus on trophic traits (Maureaud et al., 2020) holds promise for understanding how species trait structures drive non-random spatial variability in food-web structures.

The few theoretical studies addressing food-webs in space so far investigated relationships between food-web structure and sampling area (Brose et al., 2004; Galiana et al., 2018) and the implications of spatial food-web dynamics for species richness (Ryser et al., 2019, 2021). Others tested the average properties of food-webs created by simulating community assembly according to various paradigms in meta-community theory (Baiser et al., 2013) and the trophic theory of island biogeography (Gravel et al., 2011). Complementing these studies, we take a first step towards understanding the processes behind spatial variability in food-web structure and show the important role of local biotic filtering and the distribution of trophic traits in the regional species pool. We envision a number of new research avenues following our results. First, our findings on the expected distributions of species' linkage patterns and spatial variability among local food-webs are empirically testable in laboratory experiments and potentially in the field. Second, our model in its present form is minimalistic and could be easily expanded to include a more realistic simulation of food-web assembly or the effects of additional traits besides trophic ones, to investigate a broader range of drivers of food-web variability. Ultimately, such studies could investigate if human-driven biodiversity loss, typically homogenising natural communities, could also homogenise food-web structures, and, thus, ecosystem functioning across landscapes. Our study sheds a first light on the integration of spatial and trophic structures in the complex meta-communities that characterise natural ecosystems.

ACKNOWLEDGEMENTS

BB was funded by the German Research Foundation (DFG), Research Unit FOR 2716, 'Spatial community ecology in highly dynamic landscapes: from island biogeography to meta-ecosystems' [DynaCom], and the DFG Research training Group "Biological Responses

to Novel and Changing Environments" (RTG 2010). EB, RR, BG, BR, MRH, and UB acknowledge the support of the German Centre for Integrative Biodiversity Research (iDiv) Halle-Jena-Leipzig funded by the German Research Foundation (FZT 118). We thank Helmut Hillebrand and an anonymous associate editor for their helpful comments on the manuscript. Open Access funding enabled and organized by Projekt DEAL.

AUTHOR CONTRIBUTIONS

UB, RR, EB, MRH, BG, BR, CD and BB conceptualised the study. CD, DO and SS provided empirical data. CD, DO, BB, RR, EB, BG, MRH, BR, and UB analysed empirical data. BB, RR, and EB performed modelling work and analysed simulated data with contributions from UB, BG, BR, and CD. MRH created Figure 1. BB, UB, RR, and EB wrote the first draft of the manuscript, and all authors contributed substantially to revisions.

PEER REVIEW

The peer review history for this article is available at <https://publons.com/publon/10.1111/ele.13995>.

DATA AVAILABILITY STATEMENT

Forest soil environmental data are archived as part of the Biodiversity Exploratories Information System (www.bexis.uni-jena.de). Lake environmental data are published by (Sutherland, 1989). Food-web data are published by (Brose et al., 2019). The original data that were used in this study together with processed data and R code to reproduce our analyses are deposited in Dryad: <https://doi.org/10.5061/dryad.2280gb5tw>.

ORCID

Barbara Bauer  <https://orcid.org/0000-0003-2688-2788>
Emilio Berti  <https://orcid.org/0000-0001-9286-011X>
Remo Ryser  <https://orcid.org/0000-0002-3771-8986>
Benoit Gauzens  <https://orcid.org/0000-0001-7748-0362>
Myriam R. Hirt  <https://orcid.org/0000-0002-8112-2020>
Benjamin Rosenbaum  <https://orcid.org/0000-0002-2815-0874>
Ulrich Brose  <https://orcid.org/0000-0001-9156-583X>

REFERENCES

- Abrams, P.A. (1996) Limits to the similarity of competitors under hierarchical lottery competition. *The American Naturalist*, 148(1), 211–219. <http://doi.org/10.1086/285920>
- Baiser, B., Buckley, H.L., Gotelli, N.J. & Ellison, A.M. (2013) Predicting food-web structure with metacommunity models. *Oikos*, 122, 492–506.
- Barnes, A.D., Jochum, M., Lefcheck, J.S., Eisenhauer, N., Scherber, C., O'Connor, M.I. et al. (2018) Energy flux: the link between multitrophic biodiversity and ecosystem functioning. *Trends in Ecology & Evolution*, 33, 186–197.
- Barnes, A.D., Weigelt, P., Jochum, M., Ott, D., Hodapp, D., Haneda, N.F. et al. (2016) Species richness and biomass explain spatial turnover in ecosystem functioning across tropical and temperate ecosystems. *Philosophical Transactions of the Royal Society B: Biological Sciences*, 371, 20150279.
- Binzer, A., Guill, C., Rall, B.C. & Brose, U. (2016) Interactive effects of warming, eutrophication and size structure: impacts on biodiversity and food-web structure. *Global Change Biology*, 22, 220–227.
- Brose, U., Archambault, P., Barnes, A.D., Bersier, L.-F., Boy, T., Canning-Clode, J. et al. (2019) Predator traits determine food-web architecture across ecosystems. *Nature Ecology and Evolution*, 3, 919–927.
- Brose, U. & Martinez, N.D. (2004) Estimating the richness of species with variable mobility. *Oikos*, 105, 292–300.
- Brose, U., Ostling, A., Harrison, K. & Martinez, N.D. (2004) Unified spatial scaling of species and their trophic interactions. *Nature*, 428, 167–171.
- Cohen, J. (2013) *Statistical power analysis for the behavioral sciences*. London: Routledge.
- Curtsdotter, A., Binzer, A., Brose, U., de Castro, F., Ebenman, B.O., Eklöf, A. et al. (2011) Robustness to secondary extinctions: comparing trait-based sequential deletions in static and dynamic food webs. *Basic and Applied Ecology*, 12, 571–580.
- Delmas, E., Besson, M., Brice, M.-H., Burkle, L.A., Dalla Riva, G.V., Fortin, M.-J. et al. (2019) Analysing ecological networks of species interactions. *Biological Reviews*, 94(1), 16–36. <https://doi.org/10.1111/brv.12433>
- Digel, C., Curtsdotter, A., Riede, J., Klärner, B. & Brose, U. (2014) Unravelling the complex structure of forest soil food webs: higher omnivory and more trophic levels. *Oikos*, 123, 1157–1172.
- Fischer, M., Bossdorf, O., Gockel, S., Hänsel, F., Hemp, A., Hessenmöller, D. et al. (2010) Implementing large-scale and long-term functional biodiversity research: the biodiversity exploratories. *Basic and Applied Ecology*, 11, 473–485.
- Fricke, E.C. & Svensson, J.-C. (2020) Accelerating homogenization of the global plant-frugivore meta-network. *Nature*, 585, 74–78.
- Fründ, J. (2021) Dissimilarity of species interaction networks: how to partition rewiring and species turnover components. *Ecosphere*, 12, e03653.
- Galiana, N., Lurgi, M., Claramunt-López, B., Fortin, M.-J., Leroux, S., Cazelles, K. et al. (2018) The spatial scaling of species interaction networks. *Nature Ecology and Evolution*, 2, 782–790.
- Gauzens, B., Rall, B.C., Mendonça, V., Vinagre, C. & Brose, U. (2020) Biodiversity of intertidal food webs in response to warming across latitudes. *Nature Climate Change*, 10, 264–269.
- Gilbert, B. & Lechowicz, M.J. (2004) Neutrality, niches, and dispersal in a temperate forest understory. *Proceedings of the National Academy of Sciences of the United States of America*, 101, 7651–7656.
- Grainger, T.N. & Gilbert, B. (2016) Dispersal and diversity in experimental metacommunities: linking theory and practice. *Oikos*, 125, 1213–1223.
- Gravel, D., Massol, F., Canard, E., Mouillot, D. & Mouquet, N. (2011) Trophic theory of island biogeography. *Ecology Letters*, 14, 1010–1016.
- Havens, K.E. (1993) Pelagic food web structure in Adirondack Mountain, USA, lakes of varying acidity. *Canadian Journal of Fisheries and Aquatic Sciences*, 50, 149–155.
- Hirt, M.R., Grimm, V., Li, Y., Rall, B.C., Rosenbaum, B. & Brose, U. (2018) Bridging scales: allometric random walks link movement and biodiversity research. *Trends in Ecology & Evolution*, 33, 701–712.
- Hirt, M.R., Tucker, M., Müller, T., Rosenbaum, B. & Brose, U. (2020) Rethinking trophic niches: speed and body mass colimit prey space of mammalian predators. *Ecology and Evolution*, 10, 7094–7105.
- Hubbell, S.P. (2001) *The unified neutral theory of biodiversity and biogeography*. Princeton, NJ: Princeton University Press.
- Keva, O., Taipale, S.J., Hayden, B., Thomas, S.M., Vesterinen, J., Kankaala, P. et al. (2021) Increasing temperature and productivity change biomass, trophic pyramids and community-level omega-3 fatty acid content in subarctic lake food webs. *Global Change Biology*, 27, 282–296.

- Klarner, B., Ehnes, R.B., Erdmann, G., Eitzinger, B., Pollierer, M.M., Maraun, M. et al. (2014) Trophic shift of soil animal species with forest type as indicated by stable isotope analysis. *Oikos*, 123, 1173–1181.
- Laigle, I., Aubin, I., Digel, C., Brose, U., Boulangeat, I. & Gravel, D. (2018) Species traits as drivers of food web structure. *Oikos*, 127, 316–326.
- Leibold, M.A. (1998) Similarity and local co-existence of species in regional biotas. *Evolutionary Ecology*, 12, 95–110.
- Leibold, M.A. & Chase, J.M. (2018) Metacommunity ecology. *Metacommunity Ecology*, 59, 90–130.
- Lindström, E.S. & Langenheder, S. (2012) Local and regional factors influencing bacterial community assembly. *Environmental Microbiology Reports*, 4, 1–9.
- Martins, V.M., Ferreira, R.L. (2020) Limiting similarity in subterranean ecosystems: a case of niche differentiation in Elmidae (Coleoptera) from epigean and hypogean environments. *Hydrobiologia*, 847(2), 593–604. <https://doi.org/10.1007/s10750-019-04123-x>
- Massol, F., Altermatt, F., Gounand, I., Gravel, D., Leibold, M.A. & Mouquet, N. (2017) How life-history traits affect ecosystem properties: effects of dispersal in meta-ecosystems. *Oikos*, 126, 532–546.
- Maureaud, A., Andersen, K.H., Zhang, L. & Lindegren, M. (2020) Trait-based food web model reveals the underlying mechanisms of biodiversity–ecosystem functioning relationships. *Journal of Animal Ecology*, 89, 1497–1510.
- MacArthur, R. & Levins, R. (1967) The limiting similarity, convergence, and divergence of coexisting species. *The American Naturalist*, 101, 377–385.
- Menge, B.A., Gouhier, T.C., Hacker, S.D., Chan, F. & Nielsen, K.J. (2015) Are meta-ecosystems organized hierarchically? A model and test in rocky intertidal habitats. *Ecological Monographs*, 85, 213–233.
- Munoz, F., Grenié, M., Denelle, P., Taudière, A., Laroche, F., Tucker, C. et al. (2018) Ecolottery: simulating and assessing community assembly with environmental filtering and neutral dynamics in R. *Methods in Ecology and Evolution*, 9, 693–703.
- Ohlsson, M. & Eklöf, A. (2020) Spatial resolution and location impact group structure in a marine food web. *Ecology Letters*, 23, 1451–1459.
- Oksanen, L., Fretwell, S.D., Arruda, J. & Niemela, P. (1981) Exploitation ecosystems in gradients of primary productivity. *The American Naturalist*, 118, 240–261.
- Ott, D., Digel, C., Klarner, B., Maraun, M., Pollierer, M., Rall, B.C. et al. (2014) Litter elemental stoichiometry and biomass densities of forest soil invertebrates. *Oikos*, 123, 1212–1223.
- Piechnik, D.A., Lawler, S.P. & Martinez, N.D. (2008) Food-web assembly during a classic biogeographic study: species’ “trophic breadth” corresponds to colonization order. *Oikos*, 117, 665–674.
- R Core Team. (2019) *R: a language and environment for statistical computing*. Vienna, Austria: R Foundation for Statistical Computing.
- Rall, B.C., Guill, C. & Brose, U. (2008) Food-web connectance and predator interference dampen the paradox of enrichment. *Oikos*, 117, 202–213.
- Rosseel, Y. (2012) lavaan: an R package for structural equation modeling. *Journal of statistical software*, 48, 1–36.
- Ryser, R., Häussler, J., Stark, M., Brose, U., Rall, B.C. & Guill, C. (2019) The biggest losers: habitat isolation deconstructs complex food webs from top to bottom. *Proceedings of the Royal Society B: Biological Sciences*, 286, 20191177.
- Ryser, R., Hirt, M.R., Häussler, J., Gravel, D. & Brose, U. (2021) Landscape heterogeneity buffers biodiversity of simulated meta-food-webs under global change through rescue and drainage effects. *Nature Communications*, 12, 4716.
- Sutherland, J.W. (1989) Field surveys of the biota and selected water chemistry parameters in 50 Adirondack Mountain lakes. Final Report, Adirondack Biota Project, New York State Department of Environmental Conservation, Albany, NY.
- Thompson, R.M., Brose, U., Dunne, J.A., Hall, R.O., Hladz, S., Kitching, R.L. et al. (2012) Food webs: reconciling the structure and function of biodiversity. *Trends in Ecology & Evolution*, 27, 689–697.
- Tuomisto, H., Ruokolainen, K. & Yli-Halla, M. (2003) Dispersal, environment, and floristic variation of western Amazonian forests. *Science*, 299, 241–244.
- Tylianakis, J.M., Martínez-García, L.B., Richardson, S.J., Peltzer, D.A. & Dickie, I.A. (2018) Symmetric assembly and disassembly processes in an ecological network. *Ecology Letters*, 21, 896–904.
- Tylianakis, J.M. & Morris, R.J. (2017) Ecological networks across environmental gradients. *Annual Review of Ecology, Evolution, and Systematics*, 48, 25–48.
- Vergnon, R., Leijs, R., van Nes, E.H., Scheffer, M. (2013) Repeated Parallel Evolution Reveals Limiting Similarity in Subterranean Diving Beetles. *The American Naturalist*, 182(1), 67–75. <https://doi.org/10.1086/670589>
- Viana, D.S. & Chase, J.M. (2019) Spatial scale modulates the inference of metacommunity assembly processes. *Ecology*, 100, e02576.

SUPPORTING INFORMATION

Additional supporting information may be found in the online version of the article at the publisher's website.

How to cite this article: Bauer, B., Berti, E., Ryser, R., Gauzens, B., Hirt, M.R., Rosenbaum, B., et al. (2022) Biotic filtering by species' interactions constrains food-web variability across spatial and abiotic gradients. *Ecology Letters*, 25, 1225–1236. Available from: <https://doi.org/10.1111/ele.13995>

Megafauna extinctions have reduced biotic connectivity worldwide

Emilio Berti^{1,2} | Jens-Christian Svenning^{1,2}

¹Section for Ecoinformatics and Biodiversity, Department of Biology, Aarhus University, Aarhus C, Denmark

²Center for Biodiversity Dynamics in a Changing World (BIOCHANGE), Department of Biology, Aarhus University, Aarhus C, Denmark

Correspondence

Emilio Berti, Section for Ecoinformatics and Biodiversity, Department of Biology, Aarhus University, Ny, Munkegade 114, DK-8000 Aarhus C, Denmark.
 Email: emilio.berti@bio.au.dk

Funding information

Villum Fonden, Grant/Award Number: 16549; Carlsbergfondet, Grant/Award Number: CF16-0005

Editor: Kathleen Lyons

Abstract

Aim: Connectivity among ecosystems is necessary to sustain ecological processes that promote biodiversity, community stability and ecosystem resilience, such as organism and nutrient dispersal. Along with human land use and habitat fragmentation, connectivity can also be affected by faunal changes. Here, we address this issue by studying how human-driven late Quaternary extinctions and extirpations of terrestrial mammals have affected the movement capacity of assemblages, an estimate of the potential connectivity among ecosystems promoted by wildlife.

Location: Global.

Time period: Late Pleistocene to the Anthropocene.

Major taxa studied: All 4,395 (4,073 extant and 322 extinct) terrestrial mammals alive in the Late Pleistocene.

Methods: We combined macroecological estimates of home range size with range maps of current and natural geographical distributions of species to investigate how human pressure has modified natural movement capacity of terrestrial assemblages and how movement capacity will respond to future extinction and rewilling scenarios.

Results: Our results showed that 74% of average and 83% of maximum movement capacity of Late Pleistocene mammal assemblages has been lost owing to prehistorical and historical extinctions and extirpations. We also found that movement capacity will decrease further if current extinction trajectories are not averted. However, our results showed that current average and maximum movement capacity can be restored to twice their current values under a full rewilling scenario and that average, but not maximum movement capacity, will increase under a conservative rewilling scenario, that is, without restoring the largest megafauna most likely to cause major human–wildlife conflicts.

Main conclusions: Prehistorical and historical losses of megafauna have caused severe decreases in movement capacity of mammal assemblages, hence large reductions in ecosystem connectivity. Reintroductions can partly restore biotic connectivity, especially when the largest megafauna are also restored. However, natural levels of movement capacity cannot be recovered fully without including ecological replacements for extinct species in rewilling efforts.

KEY WORDS

connectivity, home range, Late Pleistocene extinctions, mammals, megafauna, rewilling

1 | INTRODUCTION

Well-connected ecosystems are more stable (Gravel, Massol, & Leibold, 2016) and resilient and sustain more biodiversity than fragmented ecosystems (Wilson, 1992), with positive effects on the delivery of ecosystem services (Allen-Wardell et al., 1998; Lundberg & Moberg, 2003). For instance, energy and nutrient exchanges among ecosystems promote habitat productivity and plant diversity (Holdo, Holt, Coughenour, & Ritchie, 2007; Tilman, 1994). Moreover, well-connected metacommunities are more stable and resilient to environmental fluctuations, recovering more rapidly from perturbations, and are less likely to undergo structural and functional shifts (Shackelford, Standish, Lindo, & Starzomski, 2018; Zhang, Takahashi, Hartvig, & Andersen, 2017).

Land-use-driven habitat fragmentation has decreased the connectivity among natural ecosystems in many cases (Haddad et al., 2015; Hansen et al., 2013), with consequences such as lowered population viability and reduced gene and energy flow (Lienert, 2004; Saunders, Hobbs, & Margules, 1991). Ecosystem connectivity is, however, not determined solely by the landscape template, but also by the biota living in it. Importantly, human land use constrains the movement of many animal species (Tucker et al., 2018). These restrictions further reduce ecosystem connectivity by preventing free movement of the biota that connect habitats and ecosystems. A more subtle way in which human activities might have affected ecosystem connectivity is through extinctions and extirpations of "megalinkers", which are species that connect ecosystems across large spatial scales and provide unique ecological functions (Lundberg & Moberg, 2003). Although our understanding of the causes and effects of landscape fragmentation on ecosystem connectivity is increasing (Haddad et al., 2015; Tucker et al., 2018), the consequences of species extinctions for ecosystem connectivity have been largely overlooked.

The rates of species extinctions suggest that a new mass extinction event is approaching (Ceballos et al., 2015). Among terrestrial mammals, extinctions have been biased towards large-bodied species (Sandom, Faurby, Sandel, & Svenning, 2014; Smith, Smith, Lyons, & Payne, 2018). Owing to their high metabolic demands and large-scale movements (Bowman, Jaeger, & Fahrig, 2002; Jetz, Carbone, Fulford, & Brown, 2004), extinctions of megafauna species (≥ 45 kg; Martin, 1984) represent a loss of species of particular importance for coupling ecosystems, for example, via seed and nutrient dispersal, and thereby for stabilizing local communities and promoting species diversity (Doughty, Wolf, & Malhi, 2013; Gravel et al., 2016; Guimarães, Galetti, & Jordano, 2008; Lundberg & Moberg, 2003; Schweiger & Svenning, 2018). Importantly, given that the selective loss of megafauna began in the Late Pleistocene (Smith et al., 2018), associated reductions in biotic connectivity have probably developed worldwide across the last 130,000 years (Doughty et al., 2013).

Here, we investigate how movement capacity of terrestrial mammal assemblages (a proxy for the potential biotic connectivity provided by the movement of individuals) has changed owing to extinctions and extirpations occurring through the last 130,000 years,

that is, from the Late Pleistocene onwards. Furthermore, we also examine how movement capacity would change under a future scenario whereby current extinction trajectories are not averted and International Union for Conservation of Nature (IUCN) threatened species critically endangered, endangered and vulnerable are not released from human pressure. Moreover, given that rewilding has been proposed as a strategy for restoring self-managing ecosystems via reintroductions of extirpated species (Svenning et al., 2016), we simulate two scenarios that can lead to a recovery of the movement capacity of assemblages, hence of biotic connectivity. In particular, we examine the recovery opportunities of movement capacity for a conservative rewilding scenario, whereby the species most likely to cause major human–wildlife conflicts (i.e., carnivores ≥ 100 kg and herbivores ≥ 500 kg) are avoided, and a full rewilding scenario, whereby all terrestrial mammals are allowed to re-expand to their natural ranges. By comparing movement capacity among scenarios, we investigate the impact of humans on biotic connectivity, possible future losses, and the potential of rewilding to mitigate and restore past connectivity losses.

2 | METHODS

2.1 | Movement capacity of mammals

Movement capacity estimates the size of the area visited by individuals of the local terrestrial mammal assemblage. Given that this estimate reflects the extent to which genes, nutrients, populations, patches, habitats and, in general, ecosystems are connected by individuals of the assemblage across space, movement capacity is a proxy for the potential ecosystem connectivity caused by mammal wildlife in natural ecosystems.

To quantify the movement capacity of terrestrial mammal assemblages, we derived, for each species, the area used by individuals during normal activities, that is, the home range (Burt, 1943). Given that metabolic demands increase with body mass, larger species require larger areas for gathering resources. Consequently, the home range scales allometrically with species body mass according to the power law: $H = aM^b$, where H (in square kilometres) is the home range, M (in grams) the species body mass, a the per biomass home range, and b the steepness of the increase of home range with body mass (Kelt & Van Vuren, 2001; Jetz et al., 2004). Previous studies have shown that coefficients a and b differ among carnivores, omnivores and herbivores (Kelt & Van Vuren, 2001): carnivores have the highest per biomass home ranges, followed by omnivores and herbivores. The steepness of the increase of home range size with body mass is also higher for carnivores than for omnivores and higher for omnivores than for herbivores.

We estimated species home ranges and performed a linear regression between home range, species body mass and diet on a previously published dataset (Kelt & Van Vuren, 2015; Figure 1, Supporting Information Appendix S1). We used the coefficients of the model to predict home ranges for all terrestrial mammals. Body

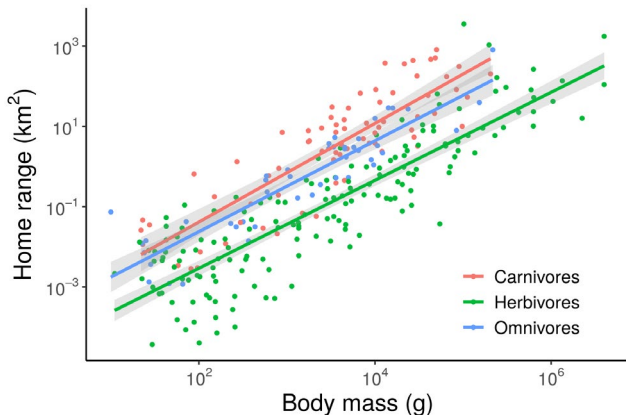


FIGURE 1 Allometric scaling of home range (km^2) with species body mass (g) in mammals. Carnivores ($n = 72$) have larger home ranges per unit of biomass than omnivores ($n = 45$), which have larger per-unit biomass home ranges than herbivores ($n = 163$). Similarly, the rate of increase of home range with body mass is higher for carnivores than for omnivores and for omnivores than for herbivores. Shaded areas show 95% confidence intervals of regression coefficients; both axes are log-transformed. Data from (Kelt & Van Vuren, 2015) and (Faurby et al., 2018) [Colour figure can be viewed at wileyonlinelibrary.com]

mass and diet of mammals were obtained from the PHYLACINE database (Faurby et al., 2018). Following previous studies (Harestad & Bunnel, 1979), we classified species as: carnivores if they had $\leq 10\%$ of their diet constituted by plants; omnivores if they had between 10 and 90% of their diet constituted by plants; and herbivores if they $\geq 90\%$ of their diet constituted by plants. To explore the sensitivity of the results to diet categorization, we ran sensitivity analyses using more strict thresholds, whereby species were classified as carnivores if they had $\leq 5\%$ of plant material in their diet, omnivores if they had $> 5\%$ and $< 95\%$, and herbivores if they had $\geq 95\%$ of plant material in their diet (Supporting Information Appendix S2). We included all 4,395 (4,073 extant + 322 extinct) terrestrial mammals alive in the Late Pleistocene in the analyses, excluding flying and aquatic mammals and genus *Homo*.

2.2 | Scenarios and movement capacity of the assemblages

Movement capacity of terrestrial mammal assemblages was estimated using the current and present-natural range maps of terrestrial mammals from the PHYLACINE database (Faurby et al., 2018). The range maps include all Late Pleistocene mammal species that were alive in the last 130,000 years and are at a 96.5 km^2 equal-area grid cell projection. PHYLACINE current ranges were derived from the IUCN polygon ranges (IUCN, 2019) and rasterized to a resolution of $96.5 \text{ km} \times 96.5 \text{ km}$ at $\pm 30^\circ$ latitude using the Behrmann equal-area projection (Faurby et al., 2018), which divides the surface of the world into cells with same area extent. The term “present-natural” refers to the state that a phenomenon

would be in today without anthropogenic (considering only *Homo sapiens*) pressure through time (Faurby & Svenning, 2015). Present-natural ranges can also be viewed as pre-*Homo sapiens* ranges adjusted for present-day climate.

PHYLACINE present-natural ranges were originally derived by Faurby & Svenning (2015) using current IUCN ranges for species unaffected by human pressure and by combining current IUCN ranges with historical distributions of species, fossil co-occurrence and known range modifications caused by humans. Importantly, co-occurrences with non-generalist species having broad climatic tolerance and geographical distribution were considered to reflect only loose associations and were excluded from range reconstruction (Faurby & Svenning 2015, Faurby et al., 2018). Notably, PHYLACINE present-natural ranges have been validated for North America previously (Faurby & Svenning 2015), showing that they are reasonably good estimates of species ranges at continental scales. Few species had, however, present-natural ranges with relatively high uncertainty and that could influence our analysis (Faurby et al., 2018). Hence, we explored the influence that potential biases in the present-natural ranges of species might have on our results using a stratified random sampling approach as the sensitivity analysis. Briefly, we sampled species from continental lists at random but assuring that final assemblages were representative of real-world mammal communities. More information can be found in the Supporting Information (Appendix S3). We also explored how our results might be affected by potential elevation biases in the PHYLACINE ranges, which, owing to their coarse resolution, include areas above the suitable elevation range of most mammals. In particular, we re-ran the analysis excluding grid cells with average elevation $\geq 2,000 \text{ m a.s.l.}$, which indicates significantly mountainous regions and approximates a conservative elevation range limit for most terrestrial mammals (Supporting Information Appendix S4).

Using the PHYLACINE range maps and species IUCN conservation status, we simulated the following five scenarios: (a) present-natural, where all extinct and extant terrestrial mammals were considered alive and occupying their present-natural ranges; (b) current, where extant species occupy their current ranges; (c) threatened species extinct, where IUCN critically endangered, endangered and vulnerable species were considered extinct and the other extant mammals occupy their current ranges; (d) conservative rewilling, where all extant terrestrial mammals, but not megacarnivores ($\geq 100 \text{ kg}$; Malhi et al., 2016) or large herbivores ($\geq 500 \text{ kg}$), could re-expand to occupy their present-natural ranges; and (e) full rewilling, where all extant terrestrial mammals could re-expand to occupy their present-natural ranges. In both rewilling scenarios, the potential for restoring the function of extinct species through ecological replacement or de-extinction was ignored (Svenning et al., 2016).

For each scenario, we estimated the mammal assemblage for each cell of the world land surface at the same resolution of the PHYLACINE range maps and calculated the average and maximum movement capacity of the assemblages. The mammal assemblage of a cell was derived as all terrestrial mammal species that were present in that cell under the scenario examined. The home ranges of the

species in the assemblage were estimated using the linear regression model between home range, body mass and diet (Figure 1). From the home range distribution of the mammal assemblage, we obtained the average and maximum assemblage home ranges, which measure the potential average and maximum movement capacity owing to mammal wildlife in that cell. Given that species are not expected to occur outside their PHYLACINE ranges, which represent the full geographical distribution of species, we did not consider movement of species outside their ranges.

Higher values of movement capacity are associated with higher movement ranges of individuals, hence higher levels of potential connectivity among ecosystems promoted by the assemblages. Both average and maximum home range were considered because some processes depend more on the average movement capacity and associated biotic connectivity (e.g., nutrient transport; Doughty et al., 2013), whereas others depend more on its maximum level (e.g., population spread of dependent species through seed dispersal; Bunney, Bond, & Henley, 2017). Both average and maximum movement capacity are species-weighted estimates, that is, they are derived as the mean and maximum values across the species in the assemblage. The reasoning is that species tend to have similar energetic effects on ecosystems at macroecological scales (White, Ernest, Kerkhoff, & Enquist, 2007), because species population density and metabolic requirements show opposite relationships with body size (Brown, Gillooly, Allen, Savage, & West, 2004; Damuth, 1981). Moreover, exceptions to this energetic equivalence rule suggest that large-bodied species have larger shares of the available resources, hence larger effects on the flow of energy and nutrients (Pedersen, Faurby, & Svenning, 2017). The mean species-weighted estimate thus reflects the general pattern of species interaction with ecosystems (White et al., 2007), whereas the maximum species-weighted estimate represents the potential disproportionate effect of large-bodied mammals (Pedersen et al., 2017). The population density of species varies across their geographical ranges depending on abiotic and biotic factors. Unfortunately, current knowledge on the patterns and drivers of this intra-range variation in density is limited (Santini, Pironon, Maiorano, & Thuiller, 2019) and not sufficient for incorporation into the macroecological modelling reported here. However, we expect that such variation in population density across geographical ranges should have only small effects overall, when aggregated across large numbers of species and interpreted at coarse geographical scales.

2.3 | Statistical analyses

To assess the change in movement capacity among scenarios, we performed multiple pairwise rank-sum tests (Mann & Whitney, 1947). The Supporting Information (Appendix S5, Table S5) summarizes the comparisons among scenarios. We corrected the significance level of the single tests using the Bonferroni correction to maintain an overall significance level of $\alpha = .01$, meaning that one contrast was significant if $p < .0014$. We also quantified the magnitude of the change among scenarios using the probabilistic sample

superiority as the effect size measure (Kerby, 2014; Ruscio, 2008), which was used to discriminate between significant but ecologically irrelevant differences and ecologically important ones (Cumming, 2013). We used the probabilistic sample superiority as the effect size statistic owing to the nonparametric distribution of the data and because of the high robustness of this effect size measure to outliers (Ruscio, 2008). Sample superiority, $P(X > Y)$, is defined as the probability that a value extracted at random from sample X will be greater than a value extracted at random from another sample, Y (Kerby, 2014). We estimated the sample superiority for the rank-sum test as the fraction of all possible pairs of values between the two samples for which the rank of one sample is higher than the other sample. We used commonly accepted values of sample superiority (Cohen, 2013; Ruscio, 2008; Sawilowsky, 2009) to classify the magnitude of the effect into small [$P(X > Y) \geq .56$], medium [$P(X > Y) \geq .64$], large [$P(X > Y) \geq .71$], very large [$P(X > Y) \geq .80$] and huge [$P(X > Y) \geq .92$]. Given that humans arrived on different continents at different times and that anthropogenic pressure was not uniform among continents (Barnosky, Koch, Feranec, Wing, & Shabel, 2004), we performed the analyses at a global scale and for each continent separately. By considering the Late Pleistocene, which represents the typical, megafauna-rich state of ecosystems for many millions of years into the past (Smith et al., 2010; Svenning et al., 2016), we used an evolutionarily relevant baseline for biotic connectivity before humans might have affected it through size-selective extinctions and extirpations (Smith et al., 2018).

All analyses were performed in the R programming language v.3.6.2 (R Core Team, 2016).

3 | RESULTS

Globally, only 26% of the average and 17% of the maximum present-natural movement capacity of the terrestrial mammal assemblages, hence of the potential ecosystem connectivity promoted by wildlife, are maintained today (Figure 2). The large effect sizes for these changes show that the prehistorical and historical megafauna extinctions have caused a severe decrease in movement capacity (Table 1). If currently threatened species also go extinct, average (but not maximum) movement capacity will decline further at the global scale. The small effect sizes attributable to these potential future losses show that projected future declines would be less pronounced than past losses. Both average and maximum movement capacity would increase markedly relative to the present if extant species could re-expand to occupy their present-natural geographical ranges. In particular, both average and maximum connectivity would double their current levels, with 52% of average and 34% of maximum present-natural movement capacity restored, under the full rewilling scenario. However, limiting the re-expansion to the smaller, less controversial megafauna (excluding carnivores ≥ 100 kg and herbivores ≥ 500 kg) would limit the restoration potential of rewilling to 45 and 24% of average and maximum present-natural movement capacity, respectively.

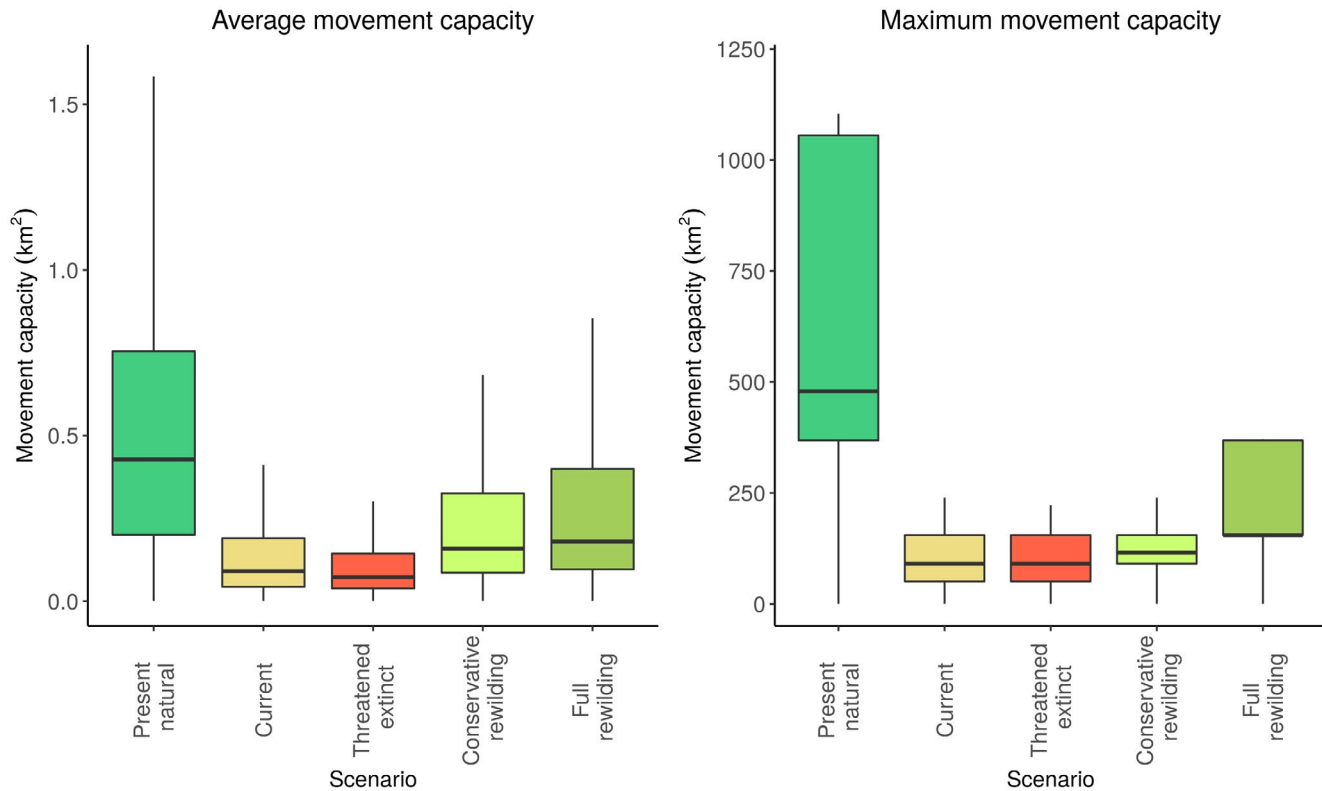


FIGURE 2 Movement capacity of terrestrial mammal assemblages under the five simulated scenarios at the global scale. Boxplots show the median (centre line), upper and lower quantiles (box limits), and 1.5 interquartile range (whiskers); outliers were removed for clarity. Average and maximum movement capacity, a proxy for average and maximum connectivity among ecosystems promoted by wildlife, were higher in the complete absence of pressure from modern humans through time (present-natural) than under current conditions. If future extinctions are not averted, average movement capacity decreased further from current conditions. Average movement capacity increased under the conservative rewilding scenarios and especially in the full rewilding scenario [Colour figure can be viewed at wileyonlinelibrary.com]

On all continents, the average and maximum movement capacity were higher in the present-natural scenario than today, with declines attributable to past extinctions having large to huge effect sizes (Table 1; Figure 3a). This decrease has not been uniform among continents: the largest decreases have occurred in Europe and the Americas, with less severe decreases in Africa, Asia and Oceania (Supporting Information Appendix S6, Figures S6.1 and S6.2). Europe has lost the largest proportion of its present-natural movement capacity through a combination of prehistoric losses and severe later range contractions, with only 9% of its natural average and 7% of its natural maximum movement capacity persisting today. In contrast, South America and Oceania had the largest loss of average and maximum movement capacity, respectively, attributable exclusively to global extinctions, reflecting severe end-Pleistocene and early Holocene losses. Moreover, Africa has maintained the biggest proportion of present-natural movement capacity of terrestrial mammal assemblages: 36% of average and 35% of maximum present-natural movement capacity area maintained currently.

When all currently threatened species are set to go extinct, average movement capacity decreases further in Africa, Asia and South America, but not in Europe, North America and Oceania (Table 1;

Figure 3b). In contrast, maximum movement capacity does not decrease significantly on any continents under this extinction scenario. In the conservative rewilding scenario, where only the smaller megafauna are allowed to re-expand to occupy their present-natural geographical ranges, average movement capacity is restored worldwide to 45% of the present-natural levels (Figure 3c). However, maximum movement capacity will not be significantly restored, but will remain similar to current conditions. When the bigger megafauna are also allowed to re-expand (the full rewilding scenario), average movement capacity increases in Africa to 75% of the present-natural value, and maximum movement capacity increases worldwide. Importantly, maximum movement capacity can be completely restored in Africa to present-natural levels and it can increase to 58% of the present-natural value in Asia (Figure 3d).

The sensitivity analyses supported the robustness of our results. In particular, results were robust to different diet categorization and potential biases in the range maps from the PHYLACINE database. Using the alternative diet categorization did not affect the results (Supporting Information Appendix S2). Moreover, results from the stratified random sampling without intra-continental range estimates showed similar general patterns (Supporting Information Appendix S3), with the only noticeable differences being a lower proportion of

TABLE 1 Proportion of movement capacity maintained by terrestrial mammal assemblages among scenarios

| Area | CU/PN | TH/CU | CRW/CU | FRW/CU | CRW/PN | FRW/PN | FRW/ CRW |
|---------------------------|-----------|-------|----------|----------|-----------|-----------|-------------|
| Average movement capacity | | | | | | | |
| Africa | 0.36**** | 0.73* | 1.68** | 2.09*** | 0.60** | 0.75* | 1.25* |
| Asia | 0.31**** | 0.74* | 1.88** | 2.25*** | 0.58** | 0.69* | 1.20 |
| Europe | 0.09***** | 0.95 | 3.33**** | 3.65**** | 0.30**** | 0.33**** | 1.09 |
| North America | 0.19**** | 0.92 | 1.76** | 1.95** | 0.33*** | 0.37*** | 1.11 |
| Oceania | 0.38*** | 0.91 | 1.47** | 1.47** | 0.56** | 0.56** | 1.00 |
| South America | 0.24**** | 0.81* | 1.19* | 1.19* | 0.28**** | 0.28**** | 1.00 |
| World | 0.26**** | 0.81* | 1.77** | 2.02** | 0.45*** | 0.52** | 1.14 |
| Maximum movement capacity | | | | | | | |
| Africa | 0.35**** | 0.68 | 1.15 | 2.15*** | 0.40**** | 0.74 | 1.87*** |
| Asia | 0.26**** | 0.61 | 1.24 | 2.23*** | 0.32**** | 0.58* | 1.80** |
| Europe | 0.07**** | 0.92 | 1.97 | 2.43 | 0.15**** | 0.18**** | 1.23 |
| North America | 0.08**** | 0.99 | 1.40 | 1.68* | 0.11**** | 0.13*** | 1.20 |
| Oceania | 0.06***** | 0.84 | 1.73 | 1.73 | 0.10**** | 0.10**** | 1.00 |
| South America | 0.19***** | 0.99 | 1.48 | 1.48 | 0.29***** | 0.29***** | 1.00 |
| World | 0.17**** | 0.77 | 1.36 | 1.97** | 0.24**** | 0.34*** | 1.45* |

Note: Superscripts show the magnitude of the change: *small, **medium, ***large, ****very large and *****huge effect sizes. Changes that were statistically non-significant ($p < .0014$, using Bonferroni correction) or that had very small effect sizes have no superscript.

Abbreviations: CRW, conservative rewinding scenario; CU, current; FRW, full rewinding scenario; PN, present-natural; TH, critically endangered, endangered and vulnerable species extinct.

average movement capacity recovered under the conservative and full rewinding scenarios for Europe and a higher proportion of maximum movement capacity recovered under the full rewinding scenario for Asia, Europe and North America (Supporting Information Appendix S3, Figure S3.2). Excluding grid cells $> 2,000$ m a.s.l. also did not affect our results (Supporting Information Appendix S4).

4 | DISCUSSION

The effects of anthropogenic pressure on ecosystem connectivity have been investigated in relationship to the consequences of landscape fragmentation on population viability (Henle, Davies, Kleyer, Margules, & Settele, 2004), community structure (Buchmann, Schurr, Nathan, & Jeltsch, 2013) and ecological functions and services (Jiang, Cheng, Li, Zhao, & Huang, 2014; Mitchell et al., 2015). Here, we show that there is another important part of the story, namely the extinctions and extirpations of mobile “megalinker” species with large movement ranges (Correia, Timóteo, Rodríguez-Echeverría, Mazars-Simon, & Heleno, 2017; Peres, Emilio, Schiotti, Desmoulière, & Levi, 2016). Our results show that extinctions of megalinkers have occurred through selective losses of megafauna since the Late Pleistocene and that the movement capacity of mammal assemblages has strongly decreased worldwide as a consequence. Such losses of movement capacity have important implications for ecosystem processes. For instance, severe decreases of movement capacity have affected mutualistic interactions, such as

seed dispersal (Guimarães et al., 2008), with plants depending on extinct megalinkers having reduced dispersal and genetic variation (Galetti et al., 2018). Moreover, our results suggest that transport of nutrients has greatly decreased worldwide owing to extinction of megafauna, probably causing long-lasting disequilibria of energy and nutrient cycles (Doughty et al., 2013). Communities will have been affected by the decreases of mammal movement capacity, because connectivity among patches strongly enhances biodiversity and resilience of metacommunities (Damschen et al., 2019; Gravel et al., 2016; Wilson, 1992). Hence, our findings suggest that ecosystems must have become increasingly unstable and vulnerable to biodiversity losses after Late Pleistocene and Holocene megafaunal extinctions. Importantly, our results show that such losses of movement capacity must have affected ecosystems globally, even in natural habitats where the landscape has not been fragmented. Our findings also show that restoration of extant mammal species to their full present-natural ranges can lead to a partial recovery of the lost movement capacity of mammal assemblages, hence the associated ecosystem processes. This recovery can be achieved through spontaneous range re-expansions and species reintroductions as part of classic reintroduction programmes or as part of trophic rewinding efforts (Perino et al., 2019; Svenning et al., 2016). Notably, we found that restoration of movement capacity would be particularly effective if the larger, more controversial megafauna were also allowed to re-occupy their present-natural geographical ranges.

Our findings are robust to possible biases in the data used, with all sensitivity analyses supporting our results. Nevertheless, given

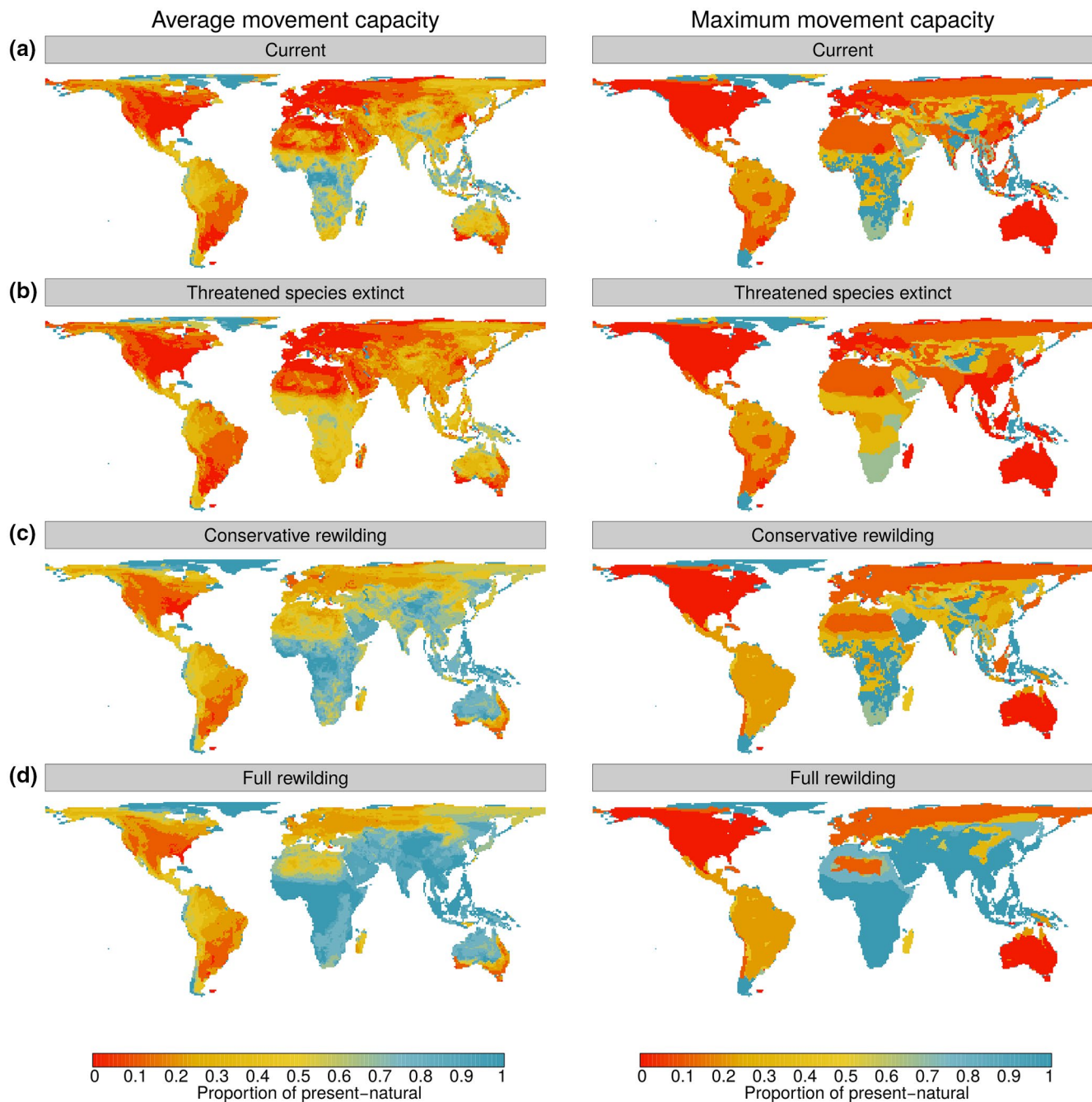


FIGURE 3 Past and future losses of movement capacity of terrestrial mammal assemblages and restoration potential of rewilling. Colours show the proportion of present-natural movement capacity that: a) has been conserved under current conditions; b) would be conserved if threatened species critically endangered, endangered, and vulnerable go extinct; c) would be restored under a conservative rewilling scenario where extant mammals, but not carnivores ≥ 100 kg or herbivores ≥ 500 kg, could re-expand to occupy their present-natural geographic ranges; and d) under a full rewilling scenario where all extant mammals could re-expand to their present-natural ranges [Colour figure can be viewed at wileyonlinelibrary.com]

the coarse-scale nature of our analyses, we would expect inaccuracies at small spatial scales. Importantly, movement capacity at finer scales is influenced by local population densities of species, environmental factors such as resource availability, and intraspecific differences among individuals (del Mar Delgado et al., 2018; Stephens, Vieira, Willis, & Carbone, 2019). For instance, individuals have larger home ranges in low-productive habitats than in

resource-rich environments (Stephens et al., 2019), with behavioural differences also determining the size of home ranges of individuals (del Mar Delgado et al., 2018). Moreover, human activities can decrease connectivity among habitat patches, for example, by creating barriers for species dispersal, thus reducing the capacity for movement of terrestrial assemblages (Tucker et al., 2018). With these caveats in mind, the sensitivity analyses show that our results are well

supported at broad spatial scales and that our findings are representative of the general losses and potential recoveries of movement capacity of terrestrial mammal assemblages, that is, given appropriate land use through increased tolerance of megafauna, conservation and restoration of natural and semi-natural areas, or passive land abandonment.

In this study, we did not take land use or other societal factors into account. The restoration estimates are thus relevant only if human–wildlife coexistence is achievable and if land use is not severely limiting wildlife movement (Tucker et al., 2018). Hence, recoveries of biotic connectivity are mainly relevant for current or future natural/semi-natural areas or areas where large-bodied species are allowed to exist in anthropogenic landscapes. Notably, such circumstances are increasingly seen in many regions globally, especially in agricultural landscapes where land abandonment has released large areas from human pressure (Ceaşu et al., 2015; Navarro & Pereira, 2015). For instance, in North America, large natural areas with high ecological integrity and landscape connectivity persist in the western USA (Belote et al., 2017), with more agricultural area also expected to be abandoned by 2040 (Ceaşu et al., 2015). Moreover, large agricultural areas are also being abandoned in Europe (Navarro & Pereira, 2015), where large-bodied species are already making a comeback owing to decreased human pressure, legislation and the implementation of conservation and restoration policies (Chapron et al., 2014; Deinet et al., 2013; Fernández, Torres, Wolf, Quintero, & Pereira, 2020). In intensely human-dominated landscapes, however, conflicts between human societies and wildlife will be likely to constrain the restoration of megafauna and associated recoveries of biotic connectivity. Yet, there is also scope for rewilding in such anthropogenic areas, for instance by reintroducing only less controversial megafauna or by achieving human–wildlife coexistence through subsidies and policies (Pedersen, Ejrnæs, Sandel, & Svenning, 2020). Opting to restore only the less controversial, smaller species will constrain the extent to which biotic connectivity is restored, but might still offer improved connectivity relative to more defaunated current situations. Notably, free-ranging large herbivores constitute important dispersal vectors in current landscapes (e.g. Vellend, Myers, Gardescu, & Marks, 2003). At the same time, there is evidence that species losses in anthropogenic landscapes can be driven by dispersal failure attributable, in part, to loss of dispersal agents (e.g. Ozinga et al., 2009). Hence, finding practical ways to enhance megafauna restoration and biotic connectivity is an important challenge for intensely human-used landscapes. Importantly, space for wildlife is projected to increase in the near future in Europe and North America, especially within or near protected areas, with an increasing number and size of wilderness areas that could support rewilding of megafauna (Ceaşu et al., 2015). The expansion of the current network of protected areas, a key component of the 2030 EU biodiversity plan (European Commission, 2020), is thus an important and promising step towards facilitating the reintroduction of megafauna and restoration of biotic connectivity. In cases where large herbivores are reintroduced into

natural areas that are fenced to reduce human–wildlife conflict (Pedersen, Ejrnæs, Sandel, & Svenning, 2020), they can at least enhance intra-reserve biotic connectivity.

Together with the spatial configuration of the landscape, the biota play a major role in promoting and maintaining ecosystem connectivity. In particular, highly mobile animals strengthen connections among ecosystems (Lundberg & Moberg, 2003). Given that mobility tends to increase with body size and that large-bodied species have suffered disproportionately from human-linked extinctions and extirpations over the last 130,000 years (Smith et al., 2018), ecosystems must have become increasingly disconnected. Our results showed that average and maximum movement capacity of terrestrial mammal assemblages have decreased worldwide following the Late Pleistocene and Holocene extinctions and extirpations among large-bodied terrestrial mammals, probably resulting in a proportional decrease of the ecosystem connectivity promoted by wildlife. Moreover, we found that average movement capacity will decrease further if future extinction trajectories are not averted. Importantly, because threatened species have decreasing population sizes (IUCN, 2019), these reductions might already be realised, in part, thereby aggravating the effects of past decreases of movement capacity for ecosystem connectivity, such as reduced nutrient transport and seed dispersal (Doughty et al., 2013; Pires, Guimarães, Galetti, & Jordano, 2018).

Among continents, Africa and Asia currently conserve higher proportions of the natural movement capacity. In Sub-Saharan Africa and South Asia, human-linked extinctions were less severe during the Late Pleistocene (Barnosky et al., 2004; Sandom et al., 2014), and these two regions conserve a higher megafauna richness today, which maintains relatively high movement capacity values within natural ecosystems. However, many of these megafauna species are threatened today and are facing extinction (IUCN, 2019), and human land use is compressing wildlife into smaller areas (Veldhuis et al., 2019); if conservation efforts fail and threatened species go extinct, movement capacity of terrestrial assemblages will decrease further in these two continents. Conversely, in both continents a re-expansion of terrestrial mammals to their present-natural ranges will restore a large proportion of the biotic connectivity that has been lost owing to anthropogenic range contractions, that is, to the extent that societal conditions would allow these recoveries. In particular, under the full rewilding scenario that included re-expansion of all megafauna (including megacarnivores ≥ 100 kg and large herbivores ≥ 500 kg) the average movement capacity will be restored to 75% of the present-natural value in Africa and to 69% in Asia, with effect sizes indicating only a small difference between full rewilding and pre-human levels. Maximum movement capacity will be restored to 58% of the present-natural levels in Asia and completely restored in Africa, highlighting the great potential of megafauna to restore movement capacity in natural ecosystems.

Europe, North America and South America have lost most of the natural movement capacity of terrestrial mammal assemblages. The Americas lost almost all large-bodied species during the megafauna extinctions following widespread human colonization

from 15,000 years ago onwards, causing the severely reduced levels of movement capacity we observe today. Moreover, average movement capacity will decrease further in South America if possible future extinctions are not averted, because four threatened megafauna species (*Hippocamelus antisensis*, *Hippocamelus bisulcus*, *Priodontes maximus* and *Tremarctos ornatus*) are responsible for promoting a relatively large proportion of the mobility of current assemblages (considering only the native species, cf. Lundgren et al., 2020). In Europe, megafauna extinctions have not been so severe compared with the Americas, and many megafauna species have survived in parts of their former ranges. However, range contractions have greatly limited the geographical distributions of these megalinkers, and their local extirpations strongly contribute to the reduced movement capacity in Europe. Extirpations are reversible, however, and Europe today has a greater potential for restoration of average movement capacity compared with the Americas, given favourable societal factors for the reintroduction of megafauna in natural and semi-natural areas and green infrastructures to assure landscape connectivity and free movement of wildlife. In particular, in the Americas current movement capacity will increase moderately under the two rewilling scenarios, whereas in Europe average movement capacity can be restored to a larger extent even under the conservative rewilling case. Although the sensitivity analyses showed slightly smaller restoration opportunities in Europe (Supporting Information Appendix S3, Figure S3.2), such recoveries of average movement capacity will still be large and ecologically important. Importantly, rewilling has already started in parts of Europe, where land abandonment, conservation efforts, rewilling projects and legal protection have promoted comebacks of several mammal species (Deinet et al., 2013; Deryabina et al., 2015). For instance, European bison (*Bison bonasus*), Eurasian elk (*Alces alces*), grey wolf (*Canis lupus*) and brown bear (*Ursus arctos*) have already been able to re-expand to part of their present-natural ranges (Chapron et al., 2014; Deinet et al., 2013). As abundance and range distribution of these species have increased, the average movement capacity of terrestrial assemblages has probably been restored, in part, in natural areas.

Contrary to average movement capacity, maximum values of the mobility of terrestrial mammal assemblages across ecosystems cannot be restored in Europe and South America under both the conservative and full rewilling scenarios. Sensitivity analyses showed, however, larger recoveries of maximum movement capacity under the full rewilling scenario in Europe, suggesting that movement capacity can be restored, in part, in this continent. In North America, a small increase in maximum connectivity can be achieved if all terrestrial mammals, including megacarnivores and large herbivores, are reintroduced in their natural ranges. The limited restoration potential of rewilling for maximum movement capacity in Europe and the Americas is attributable to the global extinction of megafauna that once lived on these three continents and that disappeared during the Late Pleistocene because of human pressure (Malhi et al., 2016), removing the most effective megalinkers from ecosystems. Extinctions are currently not

reversible, and the rewilling scenarios examined, which included only re-expansion of still living mammals into their present-natural ranges, did not consider the possibility of replacing extinct species with ecological analogue species from other regions (Svenning et al., 2016). Importantly, many non-native megafauna species have large climatic suitability ranges in Europe and the Americas (Jarvie & Svenning, 2018); the introduction of these species into areas to replace globally extinct, ecologically similar species is, therefore, the only available option for restoring maximum movement capacity to present-natural levels.

In Oceania, Australia hosted most of the megafauna richness during the Late Pleistocene. Even if almost all megafauna species went extinct after the arrival of humans in Australia (Barnosky et al., 2004), the decrease of movement capacity has been less severe compared with other continents. This result is probably biased by inaccuracies in the distribution maps of Australian mammals in the PHYLACINE database caused by sampling artefacts, probably underestimating the geographical ranges of species (Faurby & Svenning, 2015). As a result of adverse environmental factors, estimates of megafauna present-natural ranges are restricted to the relatively small, humid parts of Australia, an overly conservative estimation of their ranges, because large mammals today live in more arid Australian regions (Lundgren et al., 2020). Hence, in our model the almost complete eradication of megafauna in Australia has not resulted in an equally severe decrease in the movement capacity of mammal assemblages on the continent. We also found that, because Australian megafauna went globally extinct, average movement capacity can be restored only to a moderate extent, and maximum movement capacity cannot be restored under the considered rewilling scenarios, because these consider only extant native species. Like Europe and the Americas, the introduction of suitable non-native species as ecological replacements for extinct megafauna will be the only available option for full restoration of the movement capacity of terrestrial mammal assemblages (Jarvie & Svenning, 2018; Svenning et al., 2016). Notably, introduced feral species, which are not included in the PHYLACINE ranges, such as the dromedary (*Camelus dromedarius*), might already act as ecological replacements for the extinct native megafauna (Lundgren et al., 2020), increasing the movement capacity of assemblages and promoting connectivity among ecosystems (Muñoz-Gallego, Traveset, & Fedriani, 2019).

Overall, our results show that movement capacity of mammal assemblages has been greatly reduced by human-driven megafauna losses, inducing a decrease in the potential of wildlife to connect ecosystems across large spatial scales. Importantly, connectivity among ecosystems sustains the natural cycling of nutrients (Doughty et al., 2013), carbon sequestration (Schmitz et al., 2018), seed dispersal (Emer et al., 2018), biodiversity (Damschen et al., 2019) and forest regeneration (Elmqvist et al., 2002). Furthermore, local communities are more stable if connected into metacommunities, not only because individual species are more likely to have a lower probability of extinction (Hanski, 1998), but also because the communities can adjust rapidly to environmental perturbations (Shackelford

et al., 2018). The decrease of movement capacity in terrestrial assemblages and the decrease of the potential ecosystem connectivity maintained by wildlife might have pushed ecosystems to new states (Scheffer, Carpenter, Foley, Folke, & Walker, 2001), leading to long-lasting disequilibria that have altered the way in which ecosystems function, for example, changing vegetation dynamics (Gill, 2014), biogeochemical cycles (Doughty et al., 2013) and ecosystem resilience (Gravel et al., 2016), and have left species dependent on megafauna dispersal in slow decline or reliant on human activities for their survival (Galetti et al., 2018).

Given that humans are the main cause of this decrease, we can prevent further deterioration of movement capacity of mammal assemblages and restore part of the movement capacity that has been lost, thus strengthening ecosystem connectivity in natural areas. The protection of threatened megafauna species and their habitat is the first step in this direction. However, conservation measures alone would not be able to restore the natural connections among ecosystems, and green infrastructures that promote landscape connectivity would not restore biotic connectivity to its natural value as long as large fauna are not jointly restored. Wildlife sometimes make spontaneous comebacks (Chapron et al., 2014; Deinet et al., 2013); if we could permit extant mammals to re-expand, via spontaneous comebacks and reintroductions, and to occupy their present-natural ranges, average and maximum biotic connectivity would be restored, respectively, to half and one-third of their natural value worldwide. This restoration in itself would be a great improvement. However, to restore natural levels of biotic connectivity completely, it will be necessary to replace globally extinct megalinkers with suitable ecological substitutes (Lundgren et al., 2020; Perino et al., 2019; Svenning et al., 2016).

ACKNOWLEDGMENTS

We thank Scott Jarvie and Robert Buitenhof for comments on early versions of this manuscript and the Carlsberg Foundation for economic support of this work through the Semper Ardens project MegaPast2Future (grant CF16-0005 to J.-C.S.). J.-C.S. also considers this work a contribution to his VILLUM Investigator project "Biodiversity Dynamics in a Changing World", funded by VILLUM FONDEN (grant 16549).

DATA AVAILABILITY STATEMENT

The data that support the findings of this study are openly available in Dryad at <https://doi.org/10.5061/dryad.bp26v20> and in figshare at <https://doi.org/10.6084/m9.figshare.c.3307773.v1>. The code used to conduct the analyses is available online at <https://github.com/MegaPast2Future/megalinkers>

ORCID

Emilio Berti  <https://orcid.org/0000-0001-9286-011X>

Jens-Christian Svenning  <https://orcid.org/0000-0002-3415-0862>

REFERENCES

- Allen-Wardell, G., Bernhardt, P., Bitner, R., Burquez, A., Buchmann, S., Cane, J., ... Walker, S. (1998). The potential consequences of pollinator declines on the conservation of biodiversity and stability of food crop yields. *Conservation Biology*, 12, 8–17.
- Barnosky, A. D., Koch, P. L., Feranec, R. S., Wing, S. L., & Shabel, A. B. (2004). Assessing the causes of Late Pleistocene extinctions on the continents. *Science*, 306(5693), 70–75.
- Beloite, R. T., Dietz, M. S., Jenkins, C. N., McKinley, P. S., Irwin, G. H., Fullman, T. J., ... Aplet, G. H. (2017). Wild, connected, and diverse: building a more resilient system of protected areas. *Ecological Applications*, 27, 1050–1056.
- Bowman, J., Jaeger, J. A., & Fahrig, L. (2002). Dispersal distance of mammals is proportional to home range size. *Ecology*, 83, 2049–2055.
- Brown, J. H., Gilloly, J. F., Allen, A. P., Savage, V. M., & West, G. B. (2004). Toward a metabolic theory of ecology. *Ecology*, 85, 1771–1789.
- Buchmann, C. M., Schurr, F. M., Nathan, R., & Jeltsch, F. (2013). Habitat loss and fragmentation affecting mammal and bird communities—The role of interspecific competition and individual space use. *Ecological Informatics*, 14, 90–98.
- Bunney, K., Bond, W. J., & Henley, M. (2017). Seed dispersal kernel of the largest surviving megaherbivore—The African savanna elephant. *Biotropica*, 49, 395–401.
- Burt, W. H. (1943). Territoriality and home range concepts as applied to mammals. *Journal of Mammalogy*, 24, 346–352.
- Ceaşu, S., Hofmann, M., Navarro, L. M., Carver, S., Verburg, P. H., & Pereira, H. M. (2015). Mapping opportunities and challenges forrewilding in Europe. *Conservation Biology*, 29, 1017–1027.
- Ceballos, G., Ehrlich, P. R., Barnosky, A. D., García, A., Pringle, R. M., & Palmer, T. M. (2015). Accelerated modern human-induced species losses: Entering the sixth mass extinction. *Science Advances*, 1, e1400253.
- Chapron, G., Kaczensky, P., Linnell, J. D. C., von Arx, M., Huber, D., Andren, H., ... Boitani, L. (2014). Recovery of large carnivores in Europe's modern human-dominated landscapes. *Science*, 346(6216), 1517–1519.
- Cohen, J. (2013). *Statistical power analysis for the behavioral sciences*. London: Routledge Academic.
- Correia, M., Timóteo, S., Rodríguez-Echeverría, S., Mazars-Simon, A., & Heleno, R. (2017). Refaunation and the reinstatement of the seed-dispersal function in Gorongosa national park. *Conservation Biology*, 31, 76–85.
- Cumming, G. (2013). *Understanding the new statistics: Effect sizes, confidence intervals, and meta-analysis*. New York, NY: Routledge.
- Damschen, E. I., Brudvig, L. A., Burt, M. A., Fletcher, R. J. Jr, Haddad, N. M., Levey, D. J., ... Tewksbury, J. J. (2019). Ongoing accumulation of plant diversity through habitat connectivity in an 18-year experiment. *Science*, 365(6460), 1478–1480.
- Damuth, J. (1981). Population density and body size in mammals. *Nature*, 290(5808), 699–700.
- Deinet, S., Ieronymidou, C., McRae, L., Burfield, I. J., Foppen, R. P., & Collen, B. (2013). *Wildlife comeback in Europe: The recovery of selected mammal and bird species*. London: BirdLife International and the European Bird Census Council, ZSL.
- del Mar Delgado, M., Miranda, M., Alvarez, S. J., Gurarie, E., Fagan, W. F., Penteriani, V., ... Morales, J. M. (2018). The importance of individual variation in the dynamics of animal collective movements. *Philosophical Transactions of the Royal Society B: Biological Sciences*, 373(1746), 20170008.
- Deryabina, T. G., Kuchmel, S. V., Nagorskaya, L. L., Hinton, T. G., Beasley, J. C., Lerebours, A., & Smith, J. T. (2015). Long-term census data reveal abundant wildlife populations at Chernobyl. *Current Biology*, 25, R824–R826.
- Doughty, C. E., Wolf, A., & Malhi, Y. (2013). The legacy of the Pleistocene megafauna extinctions on nutrient availability in Amazonia. *Nature Geoscience*, 6, 761–764.
- Elmqvist, T., Wall, M., Berggren, A.-L., Blix, L., Fritioff, Å., & Rinman, U. (2002). Tropical forest reorganization after cyclone and fire

- disturbance in Samoa: Remnant trees as biological legacies. *Conservation Ecology*, 5(2), art10.
- Emer, C., Galetti, M., Pizo, M. A., Guimaraes, P. R. Jr, Moraes, S., Piratelli, A., & Jordano, P. (2018). Seed-dispersal interactions in fragmented landscapes—A metanetwork approach. *Ecology Letters*, 21, 484–493.
- European Commission (2020). *Communication from the Commission to the European Parliament, the Council, the European Economic and Social Committee and the Committee of the Regions: EU biodiversity strategy for 2030*. Retrieved from <https://eur-lex.europa.eu/legal-content/EN/TXT/?uri=CELEX:52020DC0380>
- Faurby, S., & Svenning, J.-C. (2015). Historic and prehistoric human-driven extinctions have reshaped global mammal diversity patterns. *Diversity and Distributions*, 21, 1155–1166.
- Faurby, S., Davis, M., Pedersen, R. Ø., Schowanek, S. D., Antonelli, A., & Svenning, J.-C. (2018). PHYLACINE 1.2: The phylogenetic atlas of mammal macroecology. *Ecology*, 99(11), 2626.
- Fernández, N., Torres, A., Wolf, F., Quintero, L., Pereira, H. M., & (2020). *Boosting ecological restoration for a wilder Europe* (Brochure). Nijmegen, Netherlands: Rewilding Europe. Retrieved from 10.978.39817938/57.
- Galetti, M., Moleon, M., Jordano, P., Pires, M. M., Guimaraes, P. R. Jr., Pape, T., ... Svenning, J.-C. (2018). Ecological and evolutionary legacy of megafauna extinctions. *Biological Reviews*, 93, 845–862.
- Gill, J. L. (2014). Ecological impacts of the late Quaternary megaherbivore extinctions. *New Phytologist*, 201, 1163–1169.
- Gravel, D., Massol, F., & Leibold, M. A. (2016). Stability and complexity in model meta-ecosystems. *Nature Communications*, 7(1), 12457.
- Guimaraes, P. R. Jr., Galetti, M., & Jordano, P. (2008). Seed dispersal anachronisms: Rethinking the fruits extinct megafauna ate. *PLoS One*, 3, e1745.
- Haddad, N. M., Brudvig, L. A., Clobert, J., Davies, K. F., Gonzalez, A., Holt, R. D., ... Townsend, J. R. (2015). Habitat fragmentation and its lasting impact on Earth's ecosystems. *Science Advances*, 1, e1500052.
- Hansen, M. C., Potapov, P. V., Moore, R., Hancher, M., Turubanova, S. A., Tyukavina, A., ... Townsend, J. R. G. (2013). High-resolution global maps of 21st-century forest cover change. *Science*, 342(6160), 850–853.
- Hanski, I. (1998). Metapopulation dynamics. *Nature*, 396(6706), 41–49.
- Harestad, A. S., & Bunnel, F. (1979). Home range and body weight – A reevaluation. *Ecology*, 60, 389–402.
- Henle, K., Davies, K. F., Kleyer, M., Margules, C., & Settele, J. (2004). Predictors of species sensitivity to fragmentation. *Biodiversity & Conservation*, 13, 207–251.
- Holdo, R. M., Holt, R. D., Coughenour, M. B., & Ritchie, M. E. (2007). Plant productivity and soil nitrogen as a function of grazing, migration and fire in an African savanna. *Journal of Ecology*, 95, 115–128.
- IUCN (2019). *The IUCN red list of threatened species, version 2019-3*. International Union for Conservation of Nature; Natural Resources Cambridge.
- Jarvie, S., & Svenning, J.-C. (2018). Using species distribution modeling to determine opportunities for trophic rewetting under future scenarios of climate change. *Philosophical Transactions of the Royal Society B: Biological Sciences*, 373(1761), 20170446.
- Jetz, W., Carbone, C., Fulford, J., & Brown, J. H. (2004). The scaling of animal space use. *Science*, 306(5694), 266–268.
- Jiang, P., Cheng, L., Li, M., Zhao, R., & Huang, Q. (2014). Analysis of landscape fragmentation processes and driving forces in wetlands in arid areas: A case study of the middle reaches of the Heihe river, China. *Ecological Indicators*, 46, 240–252.
- Kelt, D. A., & Van Vuren, D. H. (2001). The ecology and macroecology of mammalian home range area. *The American Naturalist*, 157, 637–645.
- Kelt, D. A., & Van Vuren, D. H. (2015). Home ranges of recent mammals. *Ecology*, 96(6), 1733.
- Kerby, D. S. (2014). The simple difference formula: An approach to teaching nonparametric correlation. *Comprehensive Psychology*, 3. Retrieved from 10.2466/11.IT.3.1
- Lienert, J. (2004). Habitat fragmentation effects on fitness of plant populations—A review. *Journal for Nature Conservation*, 12, 53–72.
- Lundberg, J., & Moberg, F. (2003). Mobile link organisms and ecosystem functioning: Implications for ecosystem resilience and management. *Ecosystems*, 6, 87–98.
- Lundgren, E. J., Ramp, D., Rowan, J., Middleton, O., Schowanek, S. D., Sanisidro, O., ... Wallach, A. D. (2020). Introduced herbivores restore Late Pleistocene ecological functions. *Proceedings of the National Academy of Sciences USA*, 117, 7871–7878.
- Malhi, Y., Doughty, C. E., Galetti, M., Smith, F. A., Svenning, J.-C., & Terborgh, J. W. (2016). Megafauna and ecosystem function from the Pleistocene to the Anthropocene. *Proceedings of the National Academy of Sciences USA*, 113, 838–846.
- Mann, H. B., & Whitney, D. R. (1947). On a test of whether one of two random variables is stochastically larger than the other. *The Annals of Mathematical Statistics*, 18, 50–60.
- Martin, P. S. (1984). Prehistoric overkill: The global model. In P. S. Martin & R. G. Klein (Eds.), *Quaternary extinctions: A prehistoric revolution* (pp. 354–403). Tucson, AZ: University of Arizona Press.
- Mitchell, M. G. E., Suarez-Castro, A. F., Martinez-Harms, M., Maron, M., McAlpine, C., Gaston, K. J., ... Rhodes, J. R. (2015). Reframing landscape fragmentation's effects on ecosystem services. *Trends in Ecology and Evolution*, 30, 190–198.
- Muñoz-Gallego, R., Traveset, A., & Fedriani, J. M. (2019). Non-native mammals are the main seed dispersers of the ancient Mediterranean palm *Chamaerops humilis* L. in the Balearic Islands: Rescuers of a lost seed dispersal service? *Frontiers in Ecology and Evolution*, 7, 161.
- Navarro, L. M., & Pereira, H. M. (2015). Rewilding abandoned landscapes in Europe. In H. M. Pereira & L. M. Navarro (Eds.), *Rewilding European landscapes* (pp. 3–23). Cham: Springer.
- Ozinga, W. A., Römermann, C., Bekker, R. M., Prinzing, A., Tamis, W. L., Schaminée, J. H., ... Bakker, J. P. (2009). Dispersal failure contributes to plant losses in NW Europe. *Ecology Letters*, 12, 66–74.
- Pedersen, P. B. M., Ejrnæs, R., Sandel, B., & Svenning, J. C. (2020). Trophic Rewilding Advancement in Anthropogenically Impacted Landscapes (TRAAIL): A framework to link conventional conservation management and rewetting. *Ambio*, 49, 231–244.
- Pedersen, R. Ø., Faurby, S., & Svenning, J. C. (2017). Shallow size-density relations within mammal clades suggest greater intra-guild ecological impact of large-bodied species. *Journal of Animal Ecology*, 86, 1205–1213.
- Peres, C. A., Emilio, T., Schietti, J., Desmoulière, S. J., & Levi, T. (2016). Dispersal limitation induces long-term biomass collapse in over-hunted Amazonian forests. *Proceedings of the National Academy of Sciences USA*, 113, 892–897.
- Perino, A., Pereira, H. M., Navarro, L. M., Fernández, N., Bullock, J. M., Ceausu, S., ... Wheeler, H. C. (2019). Rewilding complex ecosystems. *Science*, 364(6438), eaav5570.
- Pires, M. M., Guimaraes, P. R., Galetti, M., & Jordano, P. (2018). Pleistocene megafaunal extinctions and the functional loss of long-distance seed-dispersal services. *Ecography*, 41, 153–163.
- R Core Team (2016). *R: A language and environment for statistical computing*. Vienna, Austria: R Foundation for Statistical Computing. Retrieved from <http://www.R-project.org>
- Ruscio, J. (2008). A probability-based measure of effect size: Robustness to base rates and other factors. *Psychological Methods*, 13, 19–30.
- Sandom, C., Faurby, S., Sandel, B., & Svenning, J.-C. (2014). Global late Quaternary megafauna extinctions linked to humans, not climate change. *Proceedings of the Royal Society B: Biological Sciences*, 281(1787), 20133254.

- Santini, L., Pironon, S., Maiorano, L., & Thuiller, W. (2019). Addressing common pitfalls does not provide more support to geographical and ecological abundant-centre hypotheses. *Ecography*, 42, 696–705.
- Saunders, D. A., Hobbs, R. J., & Margules, C. R. (1991). Biological consequences of ecosystem fragmentation: A review. *Conservation Biology*, 5, 18–32.
- Sawilowsky, S. S. (2009). New effect size rules of thumb. *Journal of Modern Applied Statistical Methods*, 8, 597–599.
- Scheffer, M., Carpenter, S., Foley, J. A., Folke, C., & Walker, B. (2001). Catastrophic shifts in ecosystems. *Nature*, 413(6856), 591–596.
- Schmitz, O. J., Wilmers, C. C., Leroux, S. J., Doughty, C. E., Atwood, T. B., Galetti, M., ... Goetz, S. J. (2018). Animals and the zoogeochimistry of the carbon cycle. *Science*, 362(6419), eaar3213.
- Schweiger, A. H., & Svenning, J.-C. (2018). Down-sizing of dung beetle assemblages over the last 53,000 years is consistent with a dominant effect of megafauna losses. *Oikos*, 127, 1243–1250.
- Shackelford, N., Standish, R. J., Lindo, Z., & Starzomski, B. M. (2018). The role of landscape connectivity in resistance, resilience, and recovery of multi-trophic microarthropod communities. *Ecology*, 99, 1164–1172.
- Smith, F. A., Boyer, A. G., Brown, J. H., Costa, D. P., Dayan, T., Ernest, S. K. M., ... Uhen, M. D. (2010). The evolution of maximum body size of terrestrial mammals. *Science*, 330(6008), 1216–1219.
- Smith, F. A., Smith, R. E. E., Lyons, S. K., & Payne, J. L. (2018). Body size downgrading of mammals over the late Quaternary. *Science*, 360(6386), 310–313.
- Stephens, P. A., Vieira, M. V., Willis, S. G., & Carbone, C. (2019). The limits to population density in birds and mammals. *Ecology Letters*, 22, 654–663.
- Svenning, J.-C., Pedersen, P. B. M., Donlan, C. J., Ejrnaes, R., Faury, S., Galetti, M., ... Vera, F. W. M. (2016). Science for a wilder Anthropocene: Synthesis and future directions for trophic rewilding research. *Proceedings of the National Academy of Sciences USA*, 113, 898–906.
- Tilman, D. (1994). Competition and biodiversity in spatially structured habitats. *Ecology*, 75, 2–16.
- Tucker, M. A., Boehning-Gaese, K., Fagan, W. F., Fryxell, J. M., Van Moorter, B., Alberts, S. C., ... Mueller, T. (2018). Moving in the Anthropocene: Global reductions in terrestrial mammalian movements. *Science*, 359(6374), 466–469.
- Veldhuis, M. P., Ritchie, M. E., Ogutu, J. O., Morrison, T. A., Beale, C. M., Estes, A. B., ... Olff, H. (2019). Cross-boundary human impacts compromise the Serengeti-Mara ecosystem. *Science*, 363(6434), 1424–1428.
- Vellend, M., Myers, J. A., Gardescu, S., & Marks, P. L. (2003). Dispersal of Trillium seeds by deer: Implications for long-distance migration of forest herbs. *Ecology*, 84, 1067–1072.
- White, E. P., Ernest, S. M., Kerkhoff, A. J., & Enquist, B. J. (2007). Relationships between body size and abundance in ecology. *Trends in Ecology and Evolution*, 22, 323–330.
- Wilson, D. S. (1992). Complex interactions in metacommunities, with implications for biodiversity and higher levels of selection. *Ecology*, 73, 1984–2000.
- Zhang, L., Takahashi, D., Hartvig, M., & Andersen, K. H. (2017). Food-web dynamics under climate change. *Proceedings of the Royal Society B: Biological Sciences*, 284(1867), 20171772.

BIOSKETCHES

Emilio Berti is a PhD student at Aarhus University, Denmark. His work focuses on macroecological patterns in mammal communities and on the consequences of human-driven extinctions of megafauna. **Jens-Christian Svenning** is a professor of macroecology and biogeography at Aarhus University, Denmark. His research interests focus, among others, on megafauna ecology, disequilibrium dynamics, human–nature interaction and rewilding.

SUPPORTING INFORMATION

Additional Supporting Information may be found online in the Supporting Information section.

How to cite this article: Berti E, Svenning J-C. Megafauna extinctions have reduced biotic connectivity worldwide. *Global Ecol Biogeogr*. 2020;29:2131–2142. <https://doi.org/10.1111/geb.13182>



ATNr: Allometric Trophic Network models in R

Benoit Gauzens^{1,2} | Ulrich Brose^{1,2} | Eva Delmas³ | Emilio Berti^{1,2}

¹EcoNetLab, German Centre for Integrative Biodiversity Research (iDiv), Leipzig, Germany

²Institute of Biodiversity, Friedrich Schiller University, Jena, Germany

³Institut des Sciences de la Forêt Tempérée, Université du Québec en Outaouais, Ripon, Quebec, Canada

Correspondence
 Benoit Gauzens
 Email: benoit.gauzens@idiv.de

Funding information
 Deutsche Forschungsgemeinschaft,
 Grant/Award Number: FZT 118

Handling Editor: Aaron Ellison

Abstract

1. Understanding and predicting how densities of interacting species change over time has been one of the main goals of community ecology, which has become a pressing challenge in the context of global change.
2. We present the R package ATNr, which provides an implementation of different versions of Allometric Trophic Network models that simulate the biomass dynamics of trophically interacting species.
3. Relying on C++ routines, the ATNr proposes an efficient and standardised implementation of the different ATNs models.
4. By proposing a set of built in functions ready to use in a language widely used in the community of ecologists, the ATNr package offers an easy access to ATN models focusing on trophic interactions.

KEY WORDS

Allometric Trophic Network, bio-energetic, community ecology, food web, modelling, population dynamics

1 | INTRODUCTION

Understanding and predicting how densities of interacting species change over time has been one of the main goals of community ecology and that has become a pressing challenge in the context of global change, which asks for predictions of how anthropogenic and natural changes in environmental conditions will influence the functioning of future communities. Indeed, species biomass density influences ecological processes, species persistence and ecosystem stability (Gauzens et al., 2019; Kramer et al., 2018). Therefore, understanding how species' biomass changes over time is necessary for basic ecological research as well as applied management and conservation. The recent development of sequencing for food webs (Novotny et al. in press) and biomonitoring Dubart et al. (2021) offers new possibilities to compare model predictions with empirical observations to test ecological mechanisms and their associated parameter values formalised by ATN models. From a modelling perspective, the generation of time series datasets is achieved using

theoretical models that implement ordinary differential equations (ODEs) describing the rate of change in species' densities depending on their interactions with the other species in the community (Boit et al., 2012; Hudson & Reuman, 2013; Sauve & Barraquand, 2020; Volterra, 1927). Parametrising such models, however, can easily become unmanageable for large communities, due to the required quantification of species' biological rates and inter-specific interaction strengths. To solve this problem, Yodzis and Innes (1992) proposed a "bio-energetic" model that quantifies the key parameters driving species dynamics using allometric relationships with body mass (Williams et al., 2007). This greatly simplified the problem of model parametrisation, allowing the use of body mass to derive the other parameters.

The general approach of the bio-energetic model, extended by the development of metabolic theory (Brown et al., 2004), led to a new family of models, called Allometric Trophic Network models (ATNs, Martinez, 2020), as their parametrisation heavily relies on the body mass of species. In practice, allometric relationship are

This is an open access article under the terms of the [Creative Commons Attribution-NonCommercial](#) License, which permits use, distribution and reproduction in any medium, provided the original work is properly cited and is not used for commercial purposes.

© 2023 The Authors. *Methods in Ecology and Evolution* published by John Wiley & Sons Ltd on behalf of British Ecological Society.

used to relate the body mass of species to several of the biological processes driving feeding rates and species dynamics (for instance, clearance rate, handling time and metabolic rates are all function of species' body mass) and, in some cases, to estimate the presence or absence of trophic interactions (Schneider et al., 2016). Interestingly, ATNs have been shown to have the potential to represent ecosystem complexity realistically, predicting accurately community dynamics (Boit et al., 2012; Curtsdotter et al., 2019) and responses to environmental gradients (Fussmann et al., 2014). ATN models provide thus a practical compromise between biological complexity (their parametrisation is eased by the use of few easily measurable traits, i.e. species' body mass) and realism in order to model density dynamics of interacting species.

When excluding models incorporating mutualistic or economic interactions as well as ontogenetic shifts, three major ATN models are currently used today, hereafter referred as *unscaled*, *scaled* and *unscaled with nutrients*. These models differ in the possibility of including nutrient dynamics or in the way the different biological rates underlying species growth rate are determined: biological rates can be either estimated from empirical observation without further transformations or scaled to a desired level for the sake of comparability. More formally, the *unscaled* model is based on untransformed biological rates (such as clearance rate and handling time) derived using allometries. The *unscaled with nutrients* model relies on the same set of assumptions as the *scaled* version, but it explicitly includes the dynamics of nutrients and their interactions with plant species. The *scaled* model, on the other hand, scales the biological rates to the growth rate of the smallest basal species. Together, these models permit to simulate species' density dynamics in a variety of cases, for example when nutrients are explicitly accounted for and when the interest is in the untransformed biological rates or in their relative quantities. Currently, however, the application of ATN models is hindered by a lack of a standard framework, with studies using different implementations for the same underlying mathematical model.

An important step toward a common framework was recently achieved by Delmas et al. (2017), who developed a standard implementation for ATNs in the Julia programming language. Yet, this implementation focuses on a specific class of ATNs (*scaled*) and in a programming language that is unfamiliar to many ecologists. Here, we present the R package ATNr (Gauzens & Berti, 2023), which provides a standard implementation for the three major classes of ATN models. Importantly, in ATNr, the core of the calculations are evaluated by C++ routines called from within the R environment, providing a standard framework that is familiar to many ecologists while having a high computational performance.

2 | ATN MODELS

All ATN models available in ATNr describe the biomass dynamics of species by estimating their net growth rates over time. ATNr relies on two general assumptions: (i) biomass production of species are

positively affected by what they consume, that is the models are based on energetic transfers between resources and their consumers (plant species can either consume nutrients or have intrinsic logistic growth rates); (ii) loss rates of species are driven by their consumers and by metabolic costs. In this section, we cover the main aspects of the three ATN models contained in ATNr, highlighting the major differences between them. More details and the units of the different variables can be found in the package vignette (vignette("model_descriptions", package = "ATNr")).

2.1 | Species growth rate

Growth rate of species i is defined as the change of its biomass (B_i) over time: $\frac{dB_i}{dt}$. For basal species, the growth rate depends gross primary productivity minus metabolic losses and the negative effects of their consumers:

$$\frac{dB_i}{dt} = B_i r_i G_i - X_i B_i - \sum_j B_j F_{ij}, \quad (1)$$

where r_i is the maximum, mass-specific growth rate, G_i defines the proportion of r_i that is realised such as $B_i r_i G_i$ corresponds the net growth rate. X_i is the per-biomass metabolic losses, and F_{ij} is the per-biomass feeding rate of consumer j for resource i ($F_{ij} = 0$ if j does not feed on i).

For non-basal species, net intrinsic growth rate is substituted in Equation 1 by the biomass gained from resources multiplied by the assimilation efficiency of the resource j (e_j):

$$\frac{dB_i}{dt} = B_i \sum_j F_{ji} e_j - X_i B_i - \sum_j B_j F_{ij}, \quad (2)$$

These equations define allometric models as the terms involved are parametrised using scaling relationships with body mass of species (M). For instance, r_i and X_i both follow a power law that is a function of the body mass M_i of species i :

$$r_i \sim r_0 M_i^{b_r}, \quad (3)$$

$$X_i \sim X_0 M_i^{b_x}, \quad (4)$$

where r_0 and X_0 are normalisation constants and b_r and b_x the scaling exponents.

The three different versions of ATN models proposed in the package all derive from this set of equations, and only differ in how the feeding rates F_{ij} (also called functional response) are specified and how the net growth rates of basal species are calculated. For instance, a major difference in the calculation of G_i among models is whether or not the dynamic of the nutrient pool is considered.

Here, we present the formulation of feeding rate and net growth rate used by the different models and depict how the different variables are usually defined by proposing a default parametrisation based on what is used in the literature. As a convention, for all parameters that depend on both resources and consumers, like F_{ij} , the first index refers to the resource and the second to the consumer.

We provide the default parametrisations of model terms commonly used in literature in the package vignette.

2.2 | Unscaled ATN

This ATN implements the model as in Binzer et al. (2016). In ATNr, it is called *Unscaled* because the biological rates are used in their untransformed form (contrary to the *Scaled* ATN, see below). The functional response and growth rate are defined as:

$$F_{ij} = \frac{a_{ij}B_i^q}{1 + c_jB_j + \sum_k h_{kj}a_{kj}B_k^q}, \quad (5)$$

$$G_i = 1 - \frac{\sum_j \alpha_{ij}B_i}{K_i}, \quad (6)$$

where a_{ij} is the clearance rate of j on i , q is the Hill exponent determining the shape of the functional response (for type II, $q = 1$; for type III, $q \in]1, 2]$), c_j defines the intra-specific interference competition, h_{ij} is the handling time of j on i , K_i is basal species i carrying capacity, and α_{ij} is a matrix defining the ratio between inter- and intra-specific competition for resources among basal species. If α is the identity matrix, then plants growth rate only depends on intraspecific competition. If off-diagonal elements are positive values, interspecific competition is added to the model. When off-diagonal and diagonal elements are all set to one, all basal species compete for all resources. This corresponds to a scenario in which all plant species share the same resources. If the carrying capacity is the same for all species, it represents a community-level carrying capacity (the maximum total biomass of all plants).

2.3 | Scaled ATN

This ATN implements the model as in Delmas et al. (2017). It is called *Scaled* because the biological rates of species are scaled to the growth rate of the smallest basal species. The consequence of this scaling is that time is now defined as the inverse of the growth rate of the smallest producer species and the outcome of the model is to be interpreted on a relative time scale. While this may seem unnecessary complicated, it allows working at a scale adapted to the study system and to directly compare processes that happen on very different time scales (e.g. phytoplankton bloom and forest growth; Williams et al., 2007). In particular, r_i and x_i from Equation 1 and 2 are divided by the intrinsic growth rate and metabolic cost of the basal species with the smallest body mass. When species are sorted by body mass, the first one is the smallest species and: $r_i = \frac{r_i}{r_1}$, $x_i = \frac{x_i}{r_1}$. Then, it introduces the maximum feeding rate of species relative to their metabolic rate y_i , that is the ratio between maximum feeding rate and metabolic rate.

This redefinition of the variables implies a redefinition of the equations describing the dynamics of species:

$$\frac{dB_i}{dt} = B_i r_i G_i - x_i B_i - \sum_j x_j y_j B_j F_{ij}, \quad (7)$$

$$\frac{dB_i}{dt} = x_i y_i B_i \sum_j F_{ij} e_j - x_i B_i - \sum_j x_j y_j B_j F_{ij}, \quad (8)$$

The functional response and growth rate are then defined as:

$$F_{ij} = \frac{w_{ij}B_i^q}{B_0^q + c_jB_j + \sum_k w_{kj}B_k^q}, \quad (9)$$

$$G_i = 1 - \frac{\sum_j \alpha_{ij}B_i}{K_i}, \quad (10)$$

where w_{ij} is the relative consumption rate of j on i , such that $\sum_i w_{ij} = 1$.

2.4 | Unscaled ATN with nutrients

This ATN implements the model as in Schneider et al. (2016). It differs from the *Unscaled* in how the clearance rate is defined and, more importantly, by allowing the growth rate of plants to be determined by a nutrient pool dynamic, which is explicitly modelled. The functional response and growth rate are defined as:

$$F_{ij} = \frac{w_{ij}b_{ij}B_i^q}{m_i(1 + c_jB_j + \sum_k w_{kj}h_{kj}b_{kj}B_k^q)}, \quad (11)$$

$$G_i = \min_{\forall n \in \text{nutrients}} \left(\frac{N_n}{K_{ni} + N_n} \right), \quad (12)$$

where b_{ij} is the resource-specific capture coefficient, m_i is body mass of i , N_n is the concentration of nutrient n , and K_{ni} is the nutrient uptake efficiency of basal species i on nutrient n , smaller for higher efficiencies. The change of nutrient concentration over time is described by another set of differential equations:

$$\frac{dN_n}{dt} = D(S_n - N_n) - v_{ni} \sum_i r_i G_i B_i. \quad (13)$$

Here, D is the global turnover rate that determines the rate by which the nutrients are refreshed, S_n is the maximal concentration of nutrient n , and v_{ni} sets the relative content of nutrient n in plant i .

3 | USING the ATNr PACKAGE

The ATNr package consists of compiled C++ routines, which define the ATN models, together with R functions to interface with the instances of the ATNs and utility functions to solve the ordinary differential equations (ODE) and plot results. The interfacing of R and C++ makes it easy to update the parametrisation of the different models, depending on the user's goals. However, the core equations describing the dynamics of species (i.e. the ones described in the sections presenting the different models) can only be modified by updating the C++ source files. Additions of new components such as dispersion, mutualism or ontogenetic shifts would require modifying the C++ source code. Some modifications, for example, adding a term to the current equations describing species dynamics (to

incorporate mutualistic interactions or ontogenetic shifts for instance), can be achieved with relatively basic notions of C++. However, modifications adding a new component to the model, for example, a new equation describing the dynamic of an economic actor, would need to update the data structure of the package and require more advanced knowledge of C++. Still, the current C++ code and its interfacing with R could serve as a basis for future extensions.

The workflow of ATNr can be divided into four steps (Figure 1 [Table 1](#)): (1) create or get species' body masses and a food web; (2) create an instance of an ATN model; (3) initialise parameter values (potentially using the default parametrisation proposed); and (4) solve the ODE using an ODE solver.

To create an ATN model, an adjacency matrix of the food web is needed to define consumer-resource interactions together with species body masses to parametrise the ATN. The adjacency matrix can be derived from empirical data or simulated using synthetic food webs. ATNr contains two functions to generate synthetic food webs. The first is based on the niche model (Allesina et al., [2008](#); Williams & Martinez, [2000](#)): `create_niche_model(S, C)`, where S is the number

of species and C the connectance of the network. The second is based on the L matrix approach, which uses the consumer-resource body mass ratio (Schneider et al., [2016](#)): `create_Lmatrix(BM, nb_b, Ropt=100, gamma=2, th=0.01)`, where BM is a vector of species body masses, nb_n the number of basal species, $Ropt$ the optimal predator-prey body mass ratio, γ the width of the feeding kernel and th the threshold below which interactions are considered to not be realised.

From species body masses and trophic network, ATN models can be created with the functions `create_model_Scaled()` for *scaled* models, `create_model_Unscaled()` for *unscaled* models, and `create_model_Unscaled_nuts()` for *unscaled with nutrients* models. All three functions generate a C++ object (formally an instance of the C++ class) accessible within the R environment as an object of class `S4`. Once the model is created, it can be initialised to the default values used in literature (Binzer et al., [2016](#); Delmas et al., [2017](#); Schneider et al., [2016](#)) by calling `initialise_default_Scaled()`, `initialise_default_Unscaled()`, and `initialise_default_Unscaled_nuts()`.

Once the ATN models are properly created and initialised, we can solve the ODEs by specifying the integration steps and biomass of species at starting conditions as R vectors and calling an ODE solver. In ATNr, the wrapper function `lsoda_wrapper(steps, biomass, atn.model)` calls the `lsoda` solver from package `deSolve`.

As an example to summarise the general workflow of ATNr, we compute biomass dynamics for a food web of 20 species and implementing the *unscaled* ATN model. We start by creating a food web of 20 species. There are two options to generate a food web. The first one is to use the niche model (here we assumed an expected connectance of 0.3).

```
library(ATNr)
set.seed(123)
n_species <- 20 #number of species
conn <- 0.3 #connectance
fw <- create_niche_model(n_species, conn)
# The number of basal species can be calculated:
n_basal <- sum(colSums(fw) == 0)
```

We then calculate the number of basal species and species' trophic levels, which are used to obtain their body masses:

```
n_basal <- sum(colSums(fw) == 0) #number basal species
TL = TroLev(fw) #trophic levels
masses <- 1e-2 * 10 ^ (TL - 1)
```

The second option to generate a food web is to use the allometric scaling model (Schneider et al., [2016](#)), which relies on the body mass structure of a community. Therefore, it requires as an input a vector containing the body mass of species, as well as a parameter informing on the number of basal species desired. It produces a so-called L matrix which formally quantifies the probability for a consumer to successfully attack and consumer an encountered resource:

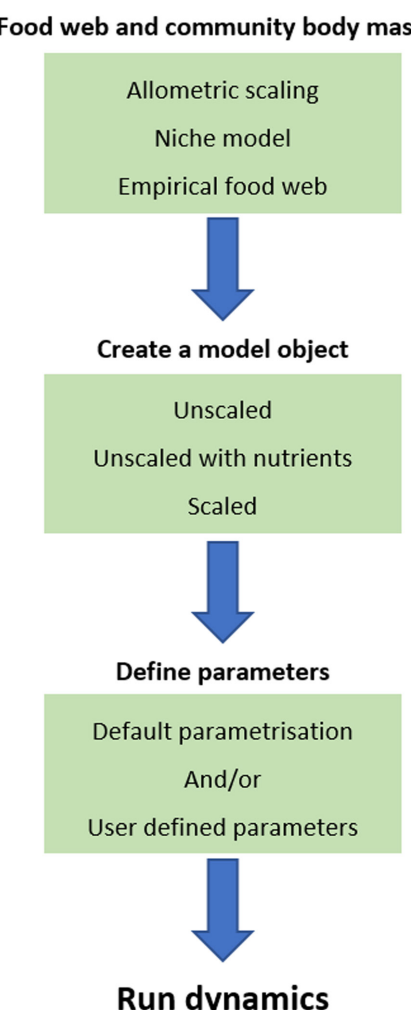


FIGURE 1 Visual representation of the workflow to simulate species dynamics on a food web. Details on the model creation and parameter definition steps can be found in [Table 1](#).

TABLE 1 Step and ATNr functions to create ATN models, specify default parametrisations and solve the biomass dynamics. nb_s is the number of species, C the connectance of the food web, BM species body mass, nb_b the number of basal species, Ropt the optimal predator-prey body mass ratio, γ the width of consumers trophic niches, th the threshold value below which there is no trophic link, fw the food web matrix, nb_n the number of nutrients, model an instance of ATN model, temperature the environmental temperature in Celsius, L.mat the L matrix, t the integration time steps, y the starting biomasses of species and nutrients, and x the matrix with ODE solutions as returned by lsoda_wrapper().

| Step | ATNr function | Required input |
|---------------------------------------|--|--|
| Create a food web | create_niche_model() create_Lmatrix() | nb_s and C BM, nb_b , Ropt, γ and th |
| Create an instance of an ATN model | create_model_Scaled() | nb_s , nb_b , BM and fw |
| | create_model_Unscaled() | nb_s , nb_b , BM and fw |
| | create_model_Scaled_nuts() | nb_s , nb_b , nb_n , BM and fw |
| Initialise parameters | initialise_default_Scaled() initialise_default_Unscaled() initialise_default_Scaled_nuts() | model model and temperature model, L.mat and temperature |
| Solve ODE and obtain biomass dynamics | lsoda_wrapper() | t, y, model |
| Plot biomass dynamics | plot_odeweb() | x, nb_s , model |

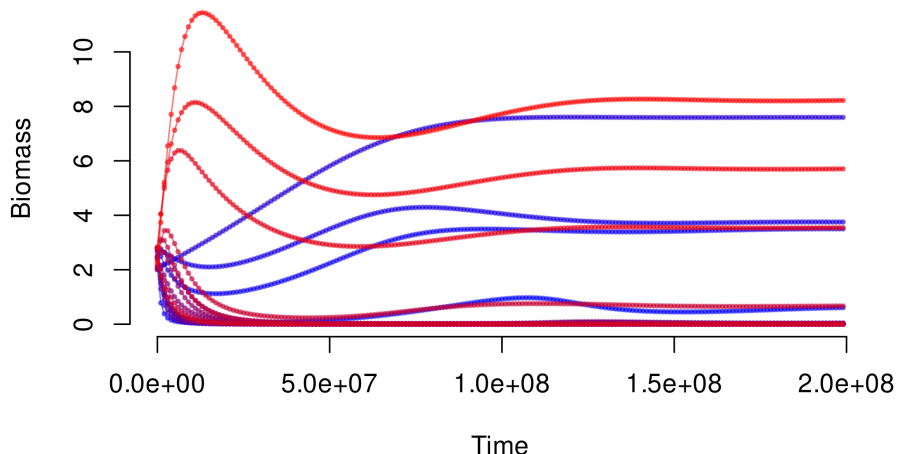


FIGURE 2 Biomass dynamics as evaluated in the example code. Colours show different species, using a gradient from blue to red based on species' ranks in the food web matrix. Dots are the solved dynamics at the pre-defined integration steps.

```
n_species <- 20
n_basal <- 5
masses <- sort(10^runif(n_species, 2, 6)) #body mass of species
L <- create_Lmatrix(masses, n_basal)
```

This L matrix can then be transformed into a binary food web:

```
fw <- L
fw[fw > 0] <- 1
```

Once the food web and species body masses are set, with one of the two methods above, we can initialise an instance of the *unscaled* ATN model, setting the parameters to their default values. Examples for the other model types can be found in the package's vignette.

```
atn.unscaled <- create_model_Unscaled(
  n_species,
  n_basal,
  masses,
  fw
```

```
)  
initialise_default_Unscaled(atn.unscaled)
```

Once we have defined starting biomasses (here randomly drawn $\in [2, 3]$) and the integration steps, the ODE can be solved:

```
biomasses <- runif(n_species, 2, 3)
times <- seq(1, 2e8, 1e6)
sol <- lsoda_wrapper(times, biomasses, atn.unscaled)
```

The variable *sol* is a *deSolve* matrix, with $n_species + 1$ columns and as many rows as the integration steps. The first column contains the integration steps and the remaining column the biomass of species at each time step. The biomass dynamics can be plotted using ATNr function plot_odeweb() (Figure 2):

```
plot_odeweb(sol, n_species)
```

From *sol*, it is straightforward to obtain several metrics with key importance for community ecology, for example the number of

species that went extinct (i.e. species for which biomass goes below a certain threshold, here 10^{-6}):

```
limit.extinction <- 1e-6
final.biomasses <- sol[nrow(sol), -1] #removing time column
sum(final.biomasses < limit.extinction) #number of species extinct
[1] 0
```

3.1 | Modifying parameters

The different initialise_default_ functions provide an easy start to run some simulations. However, an important feature of the package is that the values of the parameters used for the different models can be easily accessed and modified. Still using the model described above, it is possible to have a view of variables that can be changed with:

```
str(atn.unscaled)
```

Users can update any simulation parameters by accessing them through the \$ symbol. For instance,

```
# Define random metabolic rates:
atn.unscaled $X=runif (n_species, 0.1, 0.5)
# Using predator specific hill exponent, randomly generated:
atn.unscaled$q = runif (n_species, 0.1, 0.5)
# adding symmetric interspecific competition between plants i and j:
atn.unscaled$alpha [i, j] = 0.2
atn.unscaled$alpha [j, i] = 0.2
```

As a consequence, it is possible to entirely parametrise a model by manually defining all values instead of calling the different default initialisation functions.

4 | APPLICATIONS

To show the potential applications of ATNr, we explored two cases: (1) the effects of temperature on species persistence and (2) the paradox of enrichment. These examples are also shown in the package vignette (vignette("ATNr")).

4.1 | Effect of temperature on species persistence

ATNr makes it relatively easy to vary one parameter to assess its effect on the population dynamics. As example, we focus here on environmental temperature, which has been shown to influence biological rates of organism and to play an important role in their persistence (Gauzens et al., 2020). In ATNr, temperature can be specified in the unscaled and unscaled with nutrients models at initialisation: initialise_default_Unscaled(model, temperature) and

initialise_default_Unscaled_nuts(model, L.mat, temperature). We first create a food web using the L matrix approach:

```
set.seed(12)
n_species <- 50 #number of species
n_basal <- 20 #number of basal species
n_nut <- 2 #number of nutrients
masses <- 10 ^ c(#body mass of species
sort(runif(n_basal, 1, 3)),
sort(runif(n_species - n_basal, 2, 9))
)
L <- create_Lmatrix(masses, n_basal, # L matrix
Ropt=50, gamma=2)
fw <- L
fw[fw > 0] <- 1 #binarize L matrix
```

As we are interested in modelling nutrients explicitly, we use here the ATN model including nutrients. We thus create and initialise an instance of the *unscaled with nutrients* ATN model:

```
model <- create_model_Unscaled_nuts(
n_species, n_basal, n_nut,
masses, fw
)
```

To study the effect of temperature on species persistence, it is sufficient to loop over a temperature range and re-initialise the model instance at every iteration (Figure 3):

```
temperatures <- seq(4, 22, by=2) #temperature gradient
extinctions <- rep(NA, length(temperatures)) #store results
biomasses <- runif(n_species + n_nut, 2, 3) #starting biomasses
times <- seq(0, 100000, 100) #time steps
# loop over temperatures
```

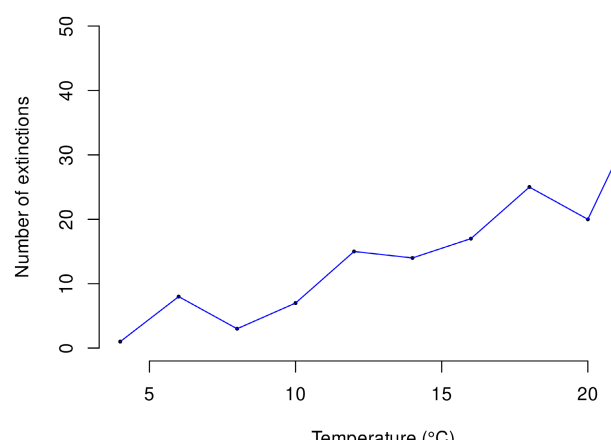


FIGURE 3 Effect of temperature on species persistence using the *unscaled with nutrients* ATN model. For increasing temperatures, more species go extinct (total species richness = 50).

```

i <- 0
for (t in temperatures) {
  model <- initialise_default_Unscaled_nuts(model, L, temperature = t)
  model $S <- rep(10, n_nut) # constant S
  # updating the value of q, same for all consumers
  model $q = rep(1.4, n_species - n_basal)
  # running simulations for the Schneider model:
  sol <- lsoda_wrapper(times, biomasses, model, verbose = FALSE)
  i <- i + 1
  # first three columns are: time, nutrient 1 and nutrient 2,
  # which are not of interest: starting from column 4.
  extinctions[i] <- sum(sol[nrow(sol), 4:ncol(sol)] < 1e-6)
}

```

Here, q and S were fixed to constant values, instead of being randomly sampled, in order to make runs at different temperature comparable.

As a note, we want to point out that in the above example there is no need to create separate instances of the ATN model, as internal parameters (temperature in this case) are changed only through `initialise_default_Unscaled_nuts()`. When this is not the case (e.g. changing number of nutrients or species), a new instance of the ATN model is needed for each simulation.

4.2 | Paradox of enrichment

Here, we want to test the paradox of enrichment, that is that increasing the carrying capacity of basal species may destabilise population dynamics (Rosenzweig, 1971), by using the *scaled* model. First, we create a food web with 10 species and initialise the model:

```

set.seed(1234)
S <- 10
fw <- create_niche_model(S, C=0.15)
TL <- TroLev(fw) #to calculate masses
masses <- 0.01 * 100 ^ (TL - 1) #body mass of species
mod <- create_model_Scaled(
  nb_s = S,
  nb_b = sum(colSums(fw) == 0),
  BM = masses,
  fw = fw
)
mod <- initialise_default_Scaled(mod)
times <- seq(0, 300, by=2) #time steps
biomasses <- runif(S, 2, 3) #starting biomasses

```

Then, we solve the system specifying the carrying capacity of basal species equal to one (`mod$K <- 1`) and then increased this to 10 (`mod$K <- 10`; Figure 4):

```

Mod $K <- 1
Sol1 <- lsoda_wrapper (times, biomasses, mod, verbose = FALSE)

```

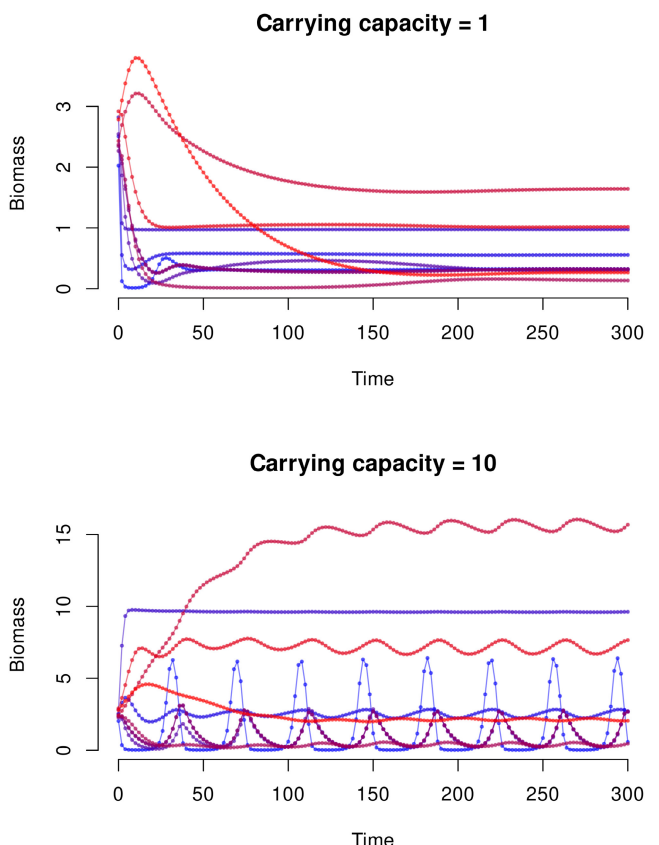


FIGURE 4 Paradox of enrichment using the *unscaled* ATN model. For higher carrying capacity of basal species ($K=10$), dynamical oscillations arise, destabilising the community. Colours correspond to different species, using a gradient from blue to red based on species' ranks in the food web matrix.

```

mod$K <- 10
sol10 <- lsoda_wrapper(times, biomasses, mod, verbose = FALSE)

```

5 | CONCLUSIONS

The R package *ATNr* provides a standardised implementation of different versions of allometric trophic network models, describing the dynamics over time of trophically interacting populations using allometric relationships. *ATNr* provides four major advantages: First, as our implementation relies on C++ routines, it allows to efficiently use ATN models in order to simulate the dynamics of interacting populations, up to several hundreds of species. Second, *ATNr* unifies the three major ATN models into a single library, providing a standardised implementation that enhances comparisons of different ATNs within a study and compatibility across several projects. Third, it provides an interface to ATN models in the R language, that is suited for a variety of users, especially in ecology. *ATNr* is a ready-to-use package and makes ATN models available also for novices, while allowing more expert users some degree of flexibility.

AUTHOR CONTRIBUTIONS

Benoit Gauzens and Emilio Berti designed the study and developed the package. Benoit Gauzens wrote the first draft of the manuscript. All authors made substantial revisions and comments to the manuscript.

ACKNOWLEDGEMENTS

Benoit Gauzens, Emilio Berti and Ulrich Brose acknowledge the support of the German Centre for Integrative Biodiversity Research (iDiv) Halle-Jena-Leipzig funded by the German Research Foundation (FZT 118). We thank Daniel Reuman for his helpful comments on the package. Open Access funding enabled and organized by Projekt DEAL.

CONFLICT OF INTEREST STATEMENT

All authors declare that they have no conflicts of interest.

PEER REVIEW

The peer review history for this article is available at <https://www.webofscience.com/api/gateway/wos/peer-review/10.1111/2041-210X.14212>.

DATA AVAILABILITY STATEMENT

The ATNr is available on CRAN: <https://cran.r-project.org/package=ATNr>. A development version can be accessed on GitHub: <https://github.com/gauzens/ATNr>. The version associated with this article is archived on Zenodo: <https://doi.org/10.5281/zenodo.8315645>.

ORCID

Benoit Gauzens  <https://orcid.org/0000-0001-7748-0362>

Emilio Berti  <https://orcid.org/0000-0001-9286-011X>

REFERENCES

- Allesina, S., Alonso, D., & Pascual, M. (2008). A general model for food web structure. *Science*, 320(5876), 658–661.
- Binzer, A., Guill, C., Rall, B. C., & Brose, U. (2016). Interactive effects of warming, eutrophication and size structure: Impacts on biodiversity and food-web structure. *Global Change Biology*, 22(1), 220–227.
- Boit, A., Martinez, N. D., Williams, R. J., & Gaedke, U. (2012). Mechanistic theory and modelling of complex food-web dynamics in lake constance. *Ecology Letters*, 15(6), 594–602.
- Brown, J. H., Gillooly, J. F., Allen, A. P., Savage, V. M., & West, G. B. (2004). Toward a metabolic theory of ecology. *Ecology*, 85(7), 1771–1789.
- Curtsdotter, A., Banks, H. T., Banks, J. E., Jonsson, M., Jonsson, T., Laubmeier, A. N., Traugott, M., & Bommarco, R. (2019). Ecosystem function in predator-prey food webs—confronting dynamic models with empirical data. *Journal of Animal Ecology*, 88(2), 196–210.
- Delmas, E., Brose, U., Gravel, D., Stouffer, D. B., & Poisot, T. (2017). Simulations of biomass dynamics in community food webs. *Methods in Ecology and Evolution*, 8(7), 881–886.
- Dubart, M., Alonso, P., Barroso-Bergada, D., Becker, N., Bethune, K., Bohan, D. A., Boury, C., Cambon, M., Canard, E., Chancerel, E., Chiquet, J., David, P., de Manincor, N., Donnet, S., Duputié, A., Facon, B., Guichoux, E., Minh, T. L., Ortiz-Martínez, S., ... Massol, F. (2021). Coupling ecological network analysis with high-throughput sequencing-based surveys: Lessons from the next-generation bio-monitoring project. *Advances in Ecological Research*, 65, 367–430.
- Fussmann, K. E., Schwarzmüller, F., Brose, U., Jousset, A., & Rall, B. C. (2014). Ecological stability in response to warming. *Nature Climate Change*, 4(3), 206–210.
- Gauzens, B., Barnes, A., Giling, D. P., Hines, J., Jochum, M., Lefcheck, J. S., Rosenbaum, B., Wang, S., & Brose, U. (2019). fluxweb: An r package to easily estimate energy fluxes in food webs. *Methods in Ecology and Evolution*, 10(2), 270–279.
- Gauzens, B., Rall, B. C., Mendonça, V., Vinagre, C., & Brose, U. (2020). Biodiversity of intertidal food webs in response to warming across latitudes. *Nature Climate Change*, 10(3), 264–269.
- Gauzens, B., & Berti, E. (2023). gauzens/ATNr: v1.1.0.
- Hudson, L. N., & Reuman, D. C. (2013). A cure for the plague of parameters: Constraining models of complex population dynamics with allometries. *Proceedings of the Royal Society B: Biological Sciences*, 280(1770), 20131901.
- Kramer, A. M., Berec, L., & Drake, J. M. (2018). Editorial: Allee effects in ecology and evolution. *Journal of Animal Ecology*, 87(1), 7–10.
- Martinez, N. D. (2020). Allometric trophic networks from individuals to socio-ecosystems: Consumer-resource theory of the ecological elephant in the room. *Frontiers in Ecology and Evolution*, 8. <https://doi.org/10.3389/fevo.2020.00092>
- Rosenzweig, M. L. (1971). Paradox of enrichment: Destabilization of exploitation ecosystems in ecological time. *Science*, 171(3969), 385–387.
- Sauve, A. M. C., & Barraquand, F. (2020). From winter to summer and back: Lessons from the parameterization of a seasonal food web model for the Białowieża forest. *Journal of Animal Ecology*, 89(7), 1628–1644.
- Schneider, F. D., Brose, U., Rall, B. C., & Guill, C. (2016). Animal diversity and ecosystem functioning in dynamic food webs. *Nature Communications*, 7(1), 1–8.
- Volterra, V. (1927). Variazioni e fluttuazioni del numero d'individui in specie animali conviventi.
- Williams, R. J., Brose, U., & Martinez, N. D. (2007). Homage to yodzis and innes 1992: Scaling up feeding-based population dynamics to complex ecological networks. In N. Rooney, K. S. McCann, & D. L. G. Noakes (Eds.), *From energetics to ecosystems: The dynamics and structure of ecological systems* (pp. 37–51). Springer.
- Williams, R. J., & Martinez, N. D. (2000). Simple rules yield complex food webs. *Nature*, 404(6774), 180–183.
- Yodzis, P., & Innes, S. (1992). Body size and consumer-resource dynamics. *The American Naturalist*, 139(6), 1151–1175.

How to cite this article: Gauzens, B., Brose, U., Delmas, E., & Berti, E. (2023). ATNr: Allometric Trophic Network models in R. *Methods in Ecology and Evolution*, 14, 2766–2773. <https://doi.org/10.1111/2041-210X.14212>